Geochimica et Cosmochimica Acta Vol. 43, pp. 1611 to 1632

0016-7037/79/1001-1611$02.00/0

Condensation and fractionation of rare earths in the solar nebula

ANDREW M. DAVIS* and LAWRENCE GROSSMAN†
Department of the Geophysical Sciences, The University of Chicago, 5734 South Ellis Avenue, Chicago, IL 60637, U.S.A.

(*Received* 18 *December* 1978; *accepted in revised form* 6 *June* 1979)

Abstract—Using the most recent thermodynamic data, we calculated the condensation behavior of REE and investigated several models to explain 'group II' REE patterns in Allende inclusions. All models involve removal of large fractions of the more refractory heavy REE in an early condensate, probably perovskite, followed by condensation of the remainder at lower temperature. BOYNTON (1975 *Geochim. Cosmochim. Acta* **39**, 569–584), found that the pattern of one such inclusion could not be fit by that of the gas remaining after *ideal* solution of REE in perovskite and, assuming the presence of only one REE component, calculated relative activity coefficients for REE in perovskite that would be needed to produce a match. In attempting to fit 20 group II patterns with this type of model, we found that these activity coefficients could not be used for most inclusions and that the relationship between ionic radius and required activity coefficients had to change rapidly and irregularly over a narrow range of perovskite removal temperature. Because this feature and the high degree of non-ideality needed are most unreasonable, we propose a different model in which two REE components control the patterns: (1) the gas remaining after removal of perovskite in which REE dissolve in *ideal* solution; (2) a material uniformly enriched in all REE. Two-component models in which solid solution of REE in perovskite is slightly non-ideal and activity coefficients vary negligibly over a narrow temperature range cannot be ruled out. By varying perovskite removal temperatures and the relative proportions of the two components, all 20 REE patterns can be satisfactorily explained.

By using a thermodynamically reasonable model, we conclude that perovskite removal occurred over a very narrow temperature range, that multiple refractory element-bearing components are present, indicating a complex history for these inclusions, and that the undeniable gas-solid fractionations that produced the REE patterns may have taken place under somewhat more reducing conditions than those of a normal solar gas.

INTRODUCTION

THERE has been considerable speculation about the origin of the fine-grained inclusions from Allende since the discovery by TANAKA and MASUDA (1973) that they contain highly fractionated abundances of the rare earth elements (REE) when compared to Cl chondrites. Tanaka and Masuda proposed that the fractionated rare earth patterns were formed by incomplete volatilization of dust followed by fractional condensation, although they did not attempt to model the process in detail.

BOYNTON (1975) calculated the condensation behavior of the rare earths and suggested a model for the origin of the REE pattern of Tanaka and Masuda's fine-grained inclusion G_p. He proposed that the more refractory heavy REE condensed in solid solution in yttrium oxide and perovskite and were removed from the gas prior to condensation of the fine-grained inclusions. Assuming ideal solid solution of REE in perovskite, Boynton calculated solid-gas distribution coefficients for the REE relative to La at 1650 K, the perovskite condensation temperature at 10^{-3} atm total pressure calculated by GROSSMAN (1972). The amount of each REE condensed was allowed to vary by varying the solid-gas distribution coefficient for La at constant temperature. Boynton found that the calculated REE pattern of the gas remaining after perovskite removal would not match that of inclusion G_p using ideal solid solution in perovskite alone. Assuming that $LnO_{1.5}$ is the compound dissolving in $CaTiO_3$, he calculated the relative activity coefficients required to make the calculated pattern match that of the inclusion. He found that there was a linear relationship between the ionic radii and the logarithms of the calculated relative activity coefficients of Sm, Gd, Dy, Er and Lu, with the relative activity coefficient of Lu ~ 35 times that of Sm.

The BOYNTON (1975) model suffers from several difficulties:

(1) It is unable to predict REE patterns as a function of temperature.

(2) In order to calculate a REE pattern, it must assume the fraction of La condensed, even though such a degree of condensation may not be allowed by thermodynamic equilibrium under the conditions assumed in the model, $T = 1650$ K and $P_T = 10^{-3}$ atm.

(3) It requires an unreasonably large degree of non-ideality of solid solution of REE in perovskite, considering the versatility of the perovskite structure and the high temperature at which perovskite condenses.

* Present address: The James Franck Institute, The University of Chicago, 5640 South Ellis Avenue, Chicago, IL 60637 U.S.A.
† Also Enrico Fermi Institute.

(4) It uses the REE pattern of the TANAKA and MASUDA (1973) inclusion to calculate thermodynamic quantities, activity coefficients, assuming that the only REE present in fine-grained inclusions are those which remained behind in the fractionated gas. Unfortunately, no other fine-grained inclusions had been analyzed at that time, so that the validity of the choice of activity coefficients could not be tested. Application of the model to a second inclusion, B-32W (BOYNTON, 1978) shows that a single set of activity coefficients cannot be used for all inclusions.

(5) It predicted that Tm would have a volatility intermediate between those of Ho and Er rather than considerably greater than that of Gd (BOYNTON, 1975, Fig. 3). Thus, a small Tm anomaly was predicted, but Tm enrichments equivalent to those of the light REE, which are now known to occur in group II inclusions, were not predicted.

Considerably more data on REE patterns in fine-grained inclusions have become available since the publication of BOYNTON (1975). MARTIN and MASON (1974) found that there are two types of REE patterns among fine-grained inclusions, with which they classified the inclusions into groups II and III. The REE patterns of the group II inclusions, like that of the inclusion analyzed by TANAKA and MASUDA (1973), are characterized by fairly uniform enrichments in light REE and lower enrichments in most heavy REE, with the enrichments dropping with increasing atomic number. Tm is enriched to nearly the same extent as the light REE and Eu and Yb are depleted to about the same degree relative to the light REE. The REE patterns of group III inclusions are characterized by uniform enrichments of nearly all REE with similar negative Eu and Yb anomalies.

There are REE analyses of group II fine-grained inclusions in TANAKA and MASUDA (1973), CONARD *et al.* (1975), CONARD (1976), MASON and MARTIN (1977), GROSSMAN and GANAPATHY (1976b), NAGASAWA *et al.* (1977) and PALME (personal communication). In addition, three coarse-grained inclusions with group II REE patterns have been analyzed: CG-5 (GROSSMAN and GANAPATHY, 1976a), 4691 (MASON and MARTIN, 1977) and CG-12 (unpublished work from this laboratory). There are also three inclusions, A-2 (CONARD, 1976), FG-16 (GROSSMAN and GANAPATHY, 1976b) and A-19 (PALME, personal communication) whose REE patterns strongly resemble those of group II inclusions, the only difference being that they have positive rather than negative Eu and Yb anomalies. We will refer to these inclusions as group IIA. The only complete REE analyses are those of CONARD (1976), shown in a figure in CONARD *et al.* (1975).

Using the most recent thermodynamic data for REE and refined solar composition condensation calculations (LATTIMER *et al.*, 1978) we have calculated the condensation behavior of the REE in order to test the BOYNTON (1975) model for all published analyses of group II inclusions and to construct a more plausible model to explain the REE patterns found in group II and group III inclusions.

METHODS OF CALCULATION

REE normalization values

All REE analyses discussed in this paper were normalized to REE abundances in Cl chondrites, since the composition of Cl chondrites is generally believed to approximate that of the total condensible matter of the solar system. The mass spectrometric isotope dilution analyses of REE in the Orgueil Cl chondrite (NAKAMURA, 1974) were adopted as normalization values for all but the four monoisotopic REE, Pr, Tb, Ho and Tm, which cannot be determined by this method. Data for the monoisotopic REE were derived from literature sources in the following way. Enrichment factors of La, Nd, Sm, Eu, Dy, Er, Yb and Lu relative to Orgueil (NAKAMURA, 1974) were calculated for each of 11 ordinary and carbonaceous chondrites analyzed by HASKIN *et al.* (1966) and for two samples of Leedey analyzed by CONARD (1976). In both of these publications, data were also given for the monoisotopic REE in each chondrite. Chauvenet's criterion (DE SOETE *et al.*, 1972) was used to reject outlying individual REE enrichment factors for each chondrite. The polyisotopic REE Ce and Gd were not used in this calculation because the enrichment factors for Ce differed from those of other REE in many of the above chondrites and the enrichment factors for Gd were consistently higher than those of other REE in the chondrites analyzed by HASKIN *et al.* (1966). The abundances in ppm of Pr, Tb, Ho and Tm in each chondrite were divided by the mean enrichment factor for the remaining REE in that chondrite. In this way, thirteen separate estimates of the Cl abundances of these four elements were made, one for each chondrite used. The means of these estimates were then calculated for each of Pr, Tb, Ho and Tm, after using Chauvenet's criterion to reject outlying values. These derived concentrations of monoisotopic REE in Cl chondrites are believed to be the best available estimates of the concentrations of these elements in the total condensible matter of the solar system. The concentrations of REE in Cl chondrites are given in Table 1, along with uncertainties for the monoisotopic REE based on the standard deviations of the values estimated above. We feel that the Cl chondrite normalization values derived here are superior to those of EVENSEN *et al.* (1978). For the polyisotopic REE, they used the mean relative abundances from several types of chondrites with the levels adjusted to match the mean for Cl chondrites. Since the Cl chondrites are generally believed to be the objects which most closely resemble solar composition in the relative abundances of all but the most volatile elements, we believe that they alone should determine the normalization values for polyisotopic REE. The EVENSEN *et al.* method for calculating normalization values for monoisotopic REE resembles ours, but their method has no provision for rejecting individual REE analyses. Several individual REE analyses are clear outliers, either due to analytical error or because they are genuine anomalies. In either case, we do not believe that these analyses should be included when calculating normalization values.

Condensation calculations

The condensation calculations were carried out in a manner similar to that of GROSSMAN (1972). For each rare earth, a mass balance equation is written,

$$N_{M_{(g)}} + N_{MO_{(g)}} + N_{MO_{1.5(s)}} = N_M^{Tot}, \quad (1)$$

where the terms represent the number of moles per liter of gaseous elemental M, gaseous monoxide, solid sesqui-

Table 1. REE concentrations* in Cl chondrites

Element	Concentration (ppm)
La	0.253
Ce	0.645
Pr	0.0965 ± 0.0032
Nd	0.476
Sm	0.154
Eu	0.0587
Gd	0.204
Tb	0.0397 ± 0.0011
Dy	0.252
Ho	0.0606 ± 0.0016
Er	0.166
Tm	0.0260 ± 0.0006
Yb	0.168
Lu	0.0253

* See text for data for Pr, Tb, Ho and Tm. Remaining data are taken from NAKAMURA (1974).

oxide and total element, respectively. The ideal gas law is used to substitute for the first term,

$$N_{M_{(g)}} = \frac{P_M}{RT}, \tag{2}$$

where P_M is the partial pressure of gaseous elemental M, R is the gas constant and T is the absolute temperature. The second term can be written in another way, using the equilibrium constant, K_1, of the reaction

$$M_{(g)} + O_{(g)} \rightleftarrows MO_{(g)}, \tag{R-1}$$

$$K_1 = \frac{P_{MO}}{P_M P_O} = \exp\left(\frac{-\Delta G_1}{RT}\right), \tag{3}$$

where ΔG_1 is the free energy of reaction (R-1), calculated from literature thermodynamic data and P_{MO} and P_O are the partial pressures of the gaseous monoxide and oxygen, respectively. An expression for N_{MO} is obtained by rearranging (3) and substituting the ideal gas law:

$$N_{MO_{(g)}} = \frac{P_M P_O K_1}{RT}. \tag{4}$$

For the case considered here, solid solution of REE in perovskite, a substitution for the third term in (1) can be calculated from the condensation behavior of perovskite and the equilibrium constant, K_2, of the reaction

$$2MO_{1.5(s)} \rightleftarrows 2M_{(g)} + 3O_{(g)}, \tag{R-2}$$

$$K_2 = \frac{P_M^2 P_O^3}{A_{MO_{1.5}}^2} = \exp\left(\frac{-\Delta G_2}{RT}\right), \tag{5}$$

where $A_{MO_{1.5}}$ is the activity of the sesquioxide in perovskite and ΔG_2 is the free energy of reaction (R-2). Writing the formula of the sesquioxide on the basis of only one cation assumes ionic behavior of M in the perovskite structure. The activity is equal to the product of the activity coefficient, $\gamma_{MO_{1.5}}$, and the mole fraction of $MO_{1.5}$ in perovskite, $X_{MO_{1.5}}$:

$$A_{MO_{1.5}} = \gamma_{MO_{1.5}} X_{MO_{1.5}}, \tag{6}$$

where

$$X_{MO_{1.5}} = \frac{N_{MO_{1.5}}}{N_{per}} \tag{7}$$

and where N_{per} is the number of moles per liter of condensed perovskite. It follows that

$$N_{MO_{1.5(s)}} = \sqrt{\frac{P_M^2 P_O^3}{\gamma_{MO_{1.5}}^2 K_2}}\, N_{per}. \tag{8}$$

Eqn (1) is then rewritten:

$$\frac{P_M}{RT} + \frac{P_M P_O K_1}{RT} + \sqrt{\frac{P_M^2 P_O^3}{\gamma_{MO_{1.5}}^2 K_2}}\, N_{per} = N_M^{Tot}. \tag{9}$$

The fraction condensed of each rare earth is given by

$$F_{cond} = \frac{N_{MO_{1.5(s)}}}{N_M^{Tot}} \tag{10}$$

which is equivalent to

$$F_{cond} = \frac{\sqrt{\frac{P_O^3}{K_2}}\,\frac{N_{per}}{\gamma_{MO_{1.5}}}}{\frac{1}{RT} + \frac{P_O K_1}{RT} + \sqrt{\frac{P_O^3}{K_2}}\,\frac{N_{per}}{\gamma}}. \tag{11}$$

Note that the degree of condensation is independent of REE cosmic abundances. The fraction remaining in the gas is given by

$$F_{gas} = 1 - F_{cond}. \tag{12}$$

Ce forms a stable, gaseous dioxide whose concentration is not negligible under high temperature, solar nebular conditions. Also, solid CeO_2 can condense in addition to solid Ce_2O_3. Thus, two additional terms, $N_{CeO_{2(g)}}$ and $N_{CeO_{2(s)}}$, the number of moles per liter of gaseous and crystalline CeO_2, respectively, must be considered in the mass balance equation for Ce. Following a derivation similar to that for (11), we find that

$$F_{cond}^{Ce} = \frac{\frac{P_O^2 N_{per}}{\gamma_{CeO_2} K_4} + \sqrt{\frac{P_O^3}{K_2}}\,\frac{N_{per}}{\gamma_{CeO_{1.5}}}}{\frac{1}{RT} + \frac{P_O K_1}{RT} + \frac{P_O^2 K_3}{RT} + \frac{P_O^2 N_{per}}{\gamma_{CeO_2} K_4} + \sqrt{\frac{P_O^3}{K_2}}\,\frac{N_{per}}{\gamma_{CeO_{1.5}}}}, \tag{13}$$

where K_3 and K_4 are the equilibrium constants for the reactions

$$Ce_{(g)} + 2O_{(g)} \rightleftarrows CeO_{2(g)} \tag{R-3}$$

and

$$CeO_{2(s)} \rightleftarrows Ce_{(g)} + 2O_{(g)}, \tag{R-4}$$

calculated from their free energies, ΔG_3 and ΔG_4, respectively.

Solid EuO can condense in addition to solid Eu_2O_3. Following a derivation similar to that of (11), we find that

$$F_{cond}^{Eu} = \frac{\frac{P_O N_{per}}{\gamma_{EuO} K_5} + \sqrt{\frac{P_O^3}{K_2}}\,\frac{N_{per}}{\gamma_{EuO_{1.5}}}}{\frac{1}{RT} + \frac{P_O K_1}{RT} + \frac{P_O N_{per}}{\gamma_{EuO} K_5} + \sqrt{\frac{P_O^3}{K_2}}\,\frac{N_{per}}{\gamma_{EuO_{1.5}}}}, \tag{14}$$

where K_5 is the equilibrium constant for the reaction

$$EuO_{(s)} \rightleftarrows Eu_{(g)} + O_{(g)} \tag{R-5}$$

calculated from its free energy, ΔG_5.

Data for the number of moles per liter of condensed perovskite and the partial pressure of oxygen at 2° tem-

perature intervals were taken from the solar nebular condensation programs at 10^{-3} atm total pressure whose results are given in LATTIMER *et al.* (1978). From eqns (11) and (12), it is clear that the only remaining quantities required to compute the REE patterns of perovskite and the gas in equilibrium with it are the thermodynamic data.

Sources of thermodynamic data

The most recent estimates of the free energies of formation of monatomic gaseous oxygen and the monatomic gaseous REE, their gaseous monoxides and their crystalline sesquioxides are those in the JANAF Tables (1977), HULTGREN *et al.* (1964 and later), AMES *et al.* (1967) and GSCHNEIDNER *et al.* (1973), respectively. The most recent estimates of the free energies of formation of gaseous and solid CeO_2 are those of ACKERMANN and RAUH (1971) and Gschneidner *et al.* (1973), respectively. Most of the data of AMES *et al.* (1967) are based on mass spectrometric measurements of the gas released from a Knudsen effusion cell in which REE sesquioxides were heated. The remaining data are based on metal-monoxide isomolecular exchange reactions for pairs of REE. The zero-degree enthalpies of formation of the gaseous REE monoxides given by Ames *et al.* are calculated from their experimental data using enthalpy data for oxygen, gaseous monatomic REE and crystalline REE sesquioxides which are different from the most recent estimates of these data. In order to use the Ames *et al.* data with newer thermodynamic data for these species, the enthalpies had to be recalculated from their experimental results. The method of recalculation is given in Appendix I and the uncertainties in these data are estimated in Appendix II. These appendices have been deposited with University Microfilms International as publication number LD 288 and can also be obtained by writing directly to the authors.

Uncertainties in calculated REE patterns

We now wish to calculate the range of REE patterns allowed by the thermodynamic data and their uncertainties for the gas remaining after perovskite removal using (11) and (12).

For monoxides with effusion-derived enthalpies, uncertainties in ΔG_2 due to uncertainties in $\Delta H^\circ_{f,O}(M_{(g)})$, $\Delta H^\circ_{f,O}(O_{(g)})$ or $\Delta H^\circ_{f,O}(M_2O_{3(s)})$ will be accompanied by uncertainties in ΔG_1, since $M_{(g)}$ and $O_{(g)}$ appear in (R-1) and all three of these enthalpies are used in deriving enthalpies for $MO_{(g)}$. Uncertainties in ΔG_1 due to other thermodynamic and experimental errors are independent of ΔG_2. We calculated the dependent and independent parts of the error in ΔG_1. The total uncertainty in ΔG_2 is given by

$$\sigma_{\Delta G_2} = \sqrt{\sigma^2_{M_2O_3} + (2\sigma_M)^2 + (3\sigma_O)^2}. \quad (15)$$

The adjustments to the individual free energies of $M_2O_{3(s)}$, $M_{(g)}$ and $O_{(g)}$ necessary to bring the value of ΔG_2 to its upper and lower error bounds allowed by (15) were calculated by assuming that the fraction of the total 1σ uncertainty is constant for each of the individual free energies and is given by:

$$\frac{\sigma_{\Delta G_2}}{\sigma_{M_2O_3} + 2\sigma_M + 3\sigma_O}. \quad (16)$$

Using these adjusted individual free energies, ΔG_1 was recalculated at the upper and lower error bounds of ΔG_2. Each of these values of ΔG_1 was then adjusted to upper and lower bounds allowed by the independent part of its uncertainty and, at each of the four values of ΔG_1, F_{gas} was calculated at 1676.5 K from (11) and (12) for each REE whose gaseous monoxide's enthalpy was derived from effusion experiments.

For REE with exchange-derived enthalpies for $M^aO_{(g)}$, adjustments of enthalpies of formation of $M^a_2O_{3(s)}$ have no effect on ΔG_1, but adjustments of those for $M^a_2O_{3(s)}$ and $M^b_{(g)}$ do have an effect, where M^a and M^b are the two REE involved in an isomolecular exchange reaction. For the purpose of simplification, the portion of the uncertainty in the adopted exchange-derived enthalpies for $M^aO_{(g)}$ independent of uncertainties in the enthalpies of species of M^b was calculated. Using these as the uncertainties in ΔG_1, F_{gas} was calculated as above for each REE whose monoxide's enthalpy was obtained from exchange data for each of the four possible combinations of upper and lower bounds of ΔG_1 and ΔG_2. For Ce, two additional species are involved in the equations, $CeO_{2(g)}$ and $CeO_{2(s)}$. No literature estimates of uncertainty in the enthalpy of $CeO_{2(g)}$ are available. Using the error estimates for the free energy of $CeO_{2(g)}$ given by GSCHNEIDNER *et al.* (1973) as the error in ΔG_4, four estimates of F_{gas} were calculated for Ce at each error bound of ΔG_4.

For each REE, the minimum and maximum F_{gas} allowed by the uncertainties in thermodynamic data were selected and plotted in Fig. 1. Because literature estimates of uncertainties in free energies of species in (R-1) and (R-2) are independent of temperature and because those calculated in Appendix II are assumed to be independent of temperature, the error bounds on ΔG_1, ΔG_2 and ΔG_4 are independent of temperature and the magnitudes of uncertainties in F_{gas}/F_{cond} are constant. For elements that are largely condensed at 1676.5 K, the uncertainties in F_{gas} will be comparable at lower temperatures. For elements that are largely in the gas phase at 1676.5 K, the uncertainties will be considerably larger at lower temperatures. The range of REE patterns allowed within thermodynamic error bounds is enormous; for example, F_{gas} for Lu at 1676.5 K can vary by a factor of 11, from 0.0033 to 0.036.

Choice of a unique set of thermodynamic data

Although many REE patterns are allowed at each temperature within our knowledge of the free energies, only one set of free energies and one REE pattern is correct at each temperature. Furthermore, the values of the free energies must vary smoothly with temperature and the degree of condensation must increase smoothly with decreasing temperature. Since we do not know the exact values of ΔG_1, ΔG_2, ΔG_3 and ΔG_4, we will determine the adjustments to the free energies required to match the REE pattern of one inclusion at a fixed temperature and apply these adjustments to the free energies at all temperatures. We will then use these adjusted free energies to see how well the REE patterns of the other inclusions can be modelled.

In the models described in this work and in BOYNTON (1975), the enrichment factors of REE in group II inclusions are determined by three quantities: (1) the fraction of each REE removed from the gas with perovskite; (2) the fraction of the amount of each REE remaining in the gas after perovskite removal which condenses along with other material to form group II inclusions; and (3) the amount of material with which these REE condense to form group II inclusions. For the heavy REE, other than Yb, the second of the above quantities is certainly one, since they are so refractory. Evidence for the complete condensation of the light REE in these inclusions comes from the high amounts of Fe, Mn, Zn and Cr in fine-grained inclusions (GROSSMAN and GANAPATHY, 1976b). Since the latter elements are all more volatile than the light REE, the light REE are assumed to have condensed completely and the second of the above quantities is assumed to be one for all REE except Eu and possibly Yb. Additional evidence for complete condensation of the light REE in group II inclusions comes from the observation that, assuming ideal solid solution, the light REE should be 95% condensed at the temperature at which spinel, an abundant mineral in all group II inclusions, first appears. The third

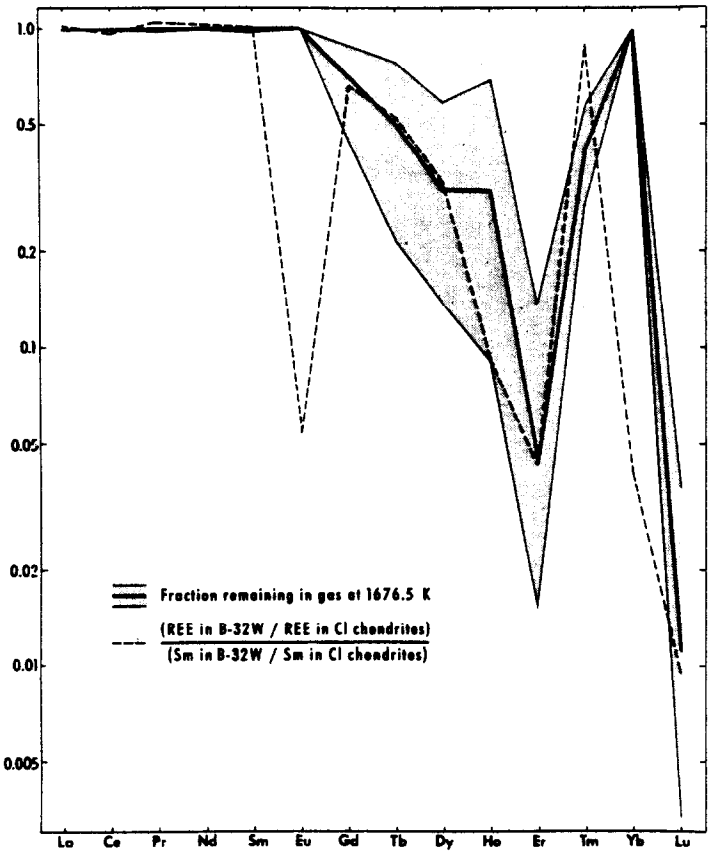

Fig. 1. Uncertainties in thermodynamic data allow a wide variety of REE patterns for the gas in equilibrium with perovskite at 1676.5 K (and at any other temperature below that at which perovskite first condenses, 1677.4 K).

of the above quantities can be eliminated as a variable by normalization to the enrichment factor of any REE except Eu and Yb. We have normalized to the enrichment factor for Sm because it is the most easily determined of all REE. By normalizing enrichment factors of other REE to that of Sm, we have transformed the problem to one of predicting relative, rather than absolute, REE patterns in inclusions and in the gas prior to condensation of the inclusions. Relative REE patterns in the theoretical calculations of the gas in equilibrium with perovskite were obtained by normalization of F_{gas} for each REE to F_{gas} for Sm.

Because there is no evidence for consistent fractionation of any single light REE from any other light REE in group II inclusions, we will not attempt to model them in detail in this paper. Since all five light REE could have coincident condensation curves within error, we have chosen ΔG_1, ΔG_2 and ΔG_4 from within their error bounds such that F_{gas} is the same for all five light REE at 1676.5 K. This will have the effect of artificially producing a flat REE pattern from La to Sm over the temperature range of interest. According to calculations using available thermodynamic data, Eu is much more volatile than the light REE and Yb is slightly more volatile than them. The depletions in Eu relative to the light REE in group II inclusions may be due to incomplete condensation of the gas remaining after perovskite removal and the enrichment of Eu in group IIA inclusions may be due to addition of a late-condensing, volatile-rich component. Because Yb is very strongly correlated with Eu in these inclusions, and is uncorrelated with either light or heavy REE, we have decided to treat it in exactly the same way as Eu, i.e. we have decoupled Yb from the detailed condensation calculations, despite the fact that it is only slightly more volatile than the light REE. Yb concentrations in these inclusions are lower than can be calculated from ideal solution models when the condensation behavior of Yb is computed in the same way as that for the other heavy REE. This has important consequences which will be discussed later in the paper.

The REE pattern used for adjustment of free energies was that of inclusion B-32W of CONARD (1976). It was chosen because analyses of all 14 REE exist for it and because, of all group II REE patterns, it is the one which most closely matches the REE pattern calculated with our unadjusted thermodynamic data assuming ideal solid solution. Free energies for Gd, Tb, Dy, Ho, Er and Lu were chosen from within their error bounds such that $F_{gas}^{REE}/F_{gas}^{Sm}$ calculated with Sm free energies adjusted as above matched the Sm-, Cl-normalized enrichment factors for these REE in B-32W at 1676.5 K. An exact match between these values could not be attained for Tm, so we have adopted the maximum allowable changes in free energies to bring its calculated value as close as possible to its measured value. The free energy adjustments computed here at 1676.5 K were applied to the free energies at all temperatures and are shown in Table 2.

DISCUSSION

One-component, ideal solution model

The composition of the gas remaining after ideal solid solution of REE in perovskite was calculated

Table 2. Adjustments to free energies required to match the REE pattern of B-32W at 1676.5 K (kcal/mol), assuming ideal solid solution of REE in perovskite (model 2). Given in italics are the adjustments required for the two-component, non-ideal solid solution model (model 3)

	ΔG_1	ΔG_2	ΔG_4
La	+3.266		
Ce	+4.983	+3.361	+2.300
Pr	+1.231		
Nd	+3.752		
Sm	−2.670		
Gd	+0.736		
	−2.400		
Tb	−0.217		
	−2.292		
Dy	−0.271		
	−1.241		
Ho	+7.029	−3.240	
	+7.053	*−3.240*	
Er	+0.217		
	+1.353		
Tm	−0.548	−3.945	
	−0.548	*−3.945*	
Lu	+0.579		
	+5.998	*−3.884*	

at several temperatures near the condensation temperature of perovskite, 1677.4 K, using the thermodynamic data as adjusted in the previous section. These calculated REE patterns are compared in Fig. 2 with the Sm-, Cl-normalized REE patterns of the three fine-grained group II inclusions and the single coarse-grained group IIA inclusion for which complete REE analyses exist (CONARD, 1976). Since the depletions in Eu and Yb relative to light REE seem to be due to incomplete condensation of these elements into group II inclusions, the fractions of these elements remaining in the gas after perovskite removal were not calculated and, for clarity, the calculated REE patterns were drawn to match the observed Eu and Yb depletions in Fig. 2.

There are several important features of the REE patterns of the gas phase in equilibrium with perovskite. Small temperature changes near the perovskite condensation temperature have tremendous effects on the calculated REE patterns, largely because the degree of condensation of perovskite is a strong function of temperature near its condensation temperature. The calculated REE patterns never cross one another, since as the temperature drops, the amounts of all REE remaining in the gas decrease. The calculated depletions of Gd, Tb, Dy, Ho, Er and Lu increase with increasing atomic number at all temperatures when B-32W is used as the standard to which thermodynamic data are fitted. All group II inclusions show this order of depletion of heavy REE. Had unfitted thermodynamic data been used, however, Ho would have been calculated to be no more depleted than Dy, as shown in Fig. 1. Tm is calculated to be less refractory than its neighbors Er and Lu, but not as volatile as the light REE, in conflict with observed group II REE patterns.

Except for Tm, which is 34% low in the calculated REE pattern, the pattern at 1676.5 K matches that of B-32W because the thermodynamic data were chosen to fit its REE pattern as closely as possible. The remaining inclusions do not match as well. B29-S1 shows a slight tendency to cross condensation curves, since the perovskite removal temperatures indicated by different REE increase progressively from 1676.2 for Gd to 1677.1 K for Lu. This effect is more pronounced for I-3, where the indicated perovskite removal temperatures increase from 1668.0 for Gd to 1677.1 K for Lu. Predicted perovskite removal temperatures for A-2 increase from 1674.6 for Gd to >1677.3 K for Lu.

Because the concentrations of different REE in the same inclusion suggest different perovskite removal temperatures, calculations of the gas composition remaining after ideal solid solution of REE in and removal from equilibrium of perovskite cannot explain the variety of REE patterns found in group II inclusions. In order to explain discrepancies between REE patterns predicted by such ideal solution calculations and that of inclusion G_p (TANAKA and MASUDA, 1973), BOYNTON (1975) assumed that the only REE component in this inclusion consists of those REE which condensed from the gas after perovskite removal. He further proposed that the heavy REE exhibit considerable non-ideality in their solid solution behavior in perovskite or other host phases and calculated the relative activity coefficients required to make the REE pattern of G_p match that of the gas remaining after removal of perovskite or other host phases with REE in non-ideal solution. We propose here two alternative models that resemble that of Boynton in their basic explanation of the observed REE fractionations, but which differ from the BOYNTON (1975) model in some important details. We will now examine the models in detail.

One-component, non-ideal solution model

The method of calculation described above remedies several of the difficulties of the BOYNTON (1975) model outlined in the Introduction. The temperature dependences of the degree of condensation of perovskite and of the partial pressure of oxygen were used here to calculate relative REE patterns of perovskite and of the gas in equilibrium with it as a function of temperature without assumptions about the degree of condensation of La. In addition, the validity of the choice of activity coefficients can be tested because many REE analyses of group II inclusions are now available.

To check the one-component, non-ideal solution model of BOYNTON (1975) for internal consistency, we used it to calculate activity coefficients for each inclusion in Fig. 2. A perovskite removal temperature was chosen for each, using the observed Sm-, Cl-normalized enrichment factor for each REE as F_{gas} for that

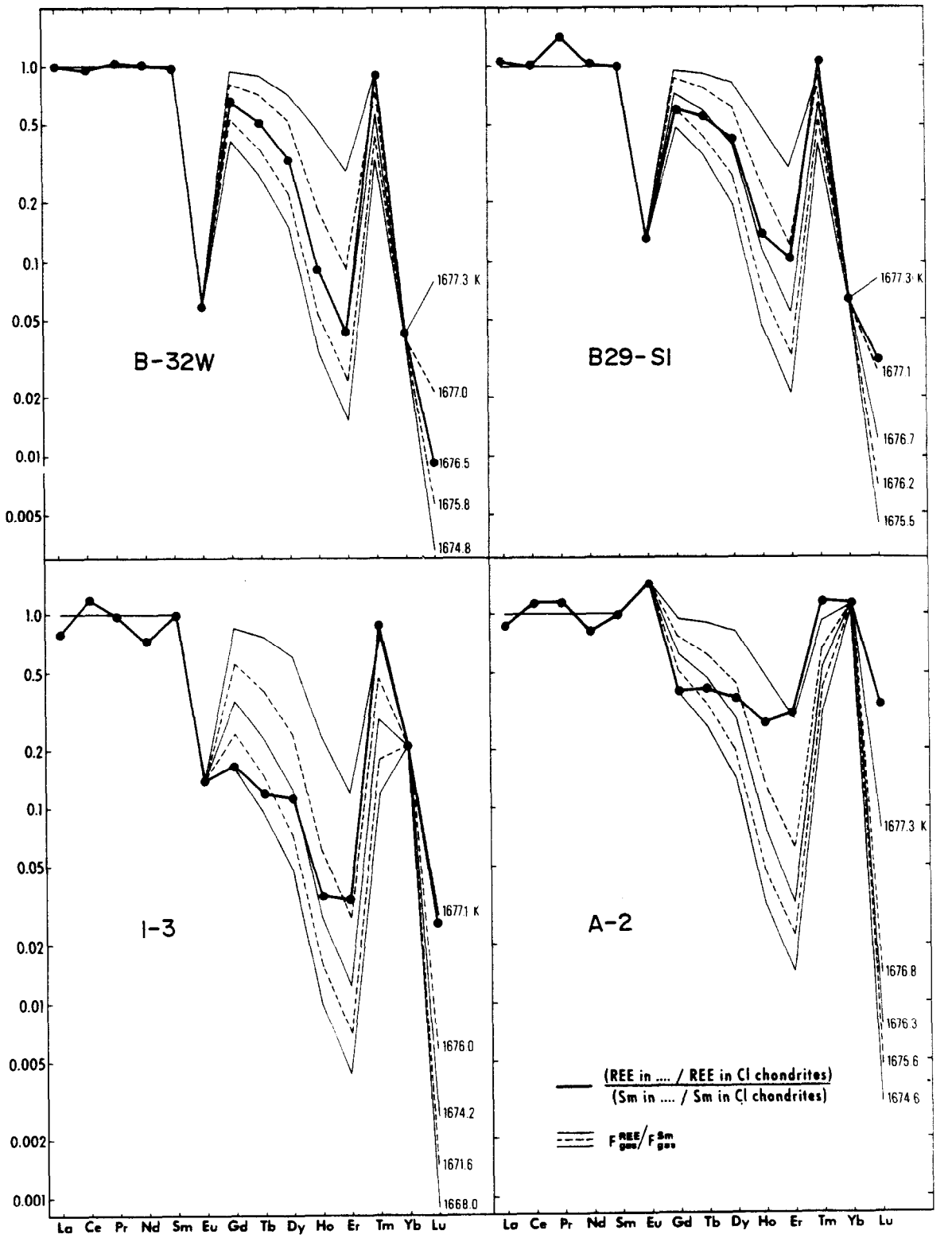

Fig. 2. Using thermodynamic data adjusted to fit inclusion B-32W in a one-component, ideal solution model, the REE patterns of B29-S1, I-3 and A-2 are not compatible with F_{gas} at any temperature. The calculated REE patterns were drawn with Eu and Yb matching the observed values for clarity.

REE divided by F_{gas}^{Sm}, assuming $\gamma_{Sm} = 1$ and solving equations (11) and (12) for γ for that REE. Although the calculated γ's vary with removal temperature, they do not vary significantly relative to one another over the temperature range considered, 1660–1677.4 K. We found that a single set of γ's would not fit all of these inclusions and that the differences between the γ's necessary to fit different inclusions were well beyond those allowed by uncertainties in the thermodynamic data.

Assuming that the gas remaining after perovskite removal was the only REE-bearing component in inclusion G_p (TANAKA and MASUDA, 1973), BOYNTON (1975) found that the best fit was obtained when there was a linear relationship between ionic radius and the logarithm of the relative activity coefficient and when γ_{Lu} was approximately 35 times γ_{Sm}. BOYNTON (1978) applied this model to inclusion B-32W (CONARD, 1976) with the same assumptions and thermodynamic data. He found that the best fit was achieved with the same functional relationship between ionic radius and activity coefficient but with γ_{Lu} only 9 times γ_{Sm}.

Although uncertainties in thermodynamic data cause large uncertainties in F_{gas} (Fig. 1), there must be a unique set of thermodynamic data which applies to all calculations. This holds not only for K_1 and K_2 but also for activity coefficients, both relative and absolute. A crucial test of the BOYNTON (1975) model is to see if a single set of relative activity coefficients can be applied to all group II inclusions, assuming that their REE patterns are controlled by a narrow range of perovskite removal temperatures. Both our calculations and those of BOYNTON (1975, 1978) show that the BOYNTON (1975) model definitely fails this test. The next question to be considered is whether different inclusions might have been affected by such widely differing perovskite removal temperatures that the required differences in relative activity coefficient functions are reasonable.

Temperature variation of the activity coefficient vs ionic radius relationship. Using thermodynamic data adjusted to fit B-32W with ideal solution at 1676.5 K, the activity coefficients required to match observed heavy REE enrichment factors can be calculated for any inclusion as a function of temperature, assuming a value for γ_{Sm}. The results of such calculations where $\gamma_{Sm} = 1$ are plotted as a function of ionic radius in Fig. 3 for B29-S1, for example. BOYNTON (1975) suggested that activity coefficients for solid solution of REE in the high temperature host phase, which he believed to be perovskite, are constant from La to Nd and that log γ increases linearly with decreasing ionic radius from Sm to Lu. It is clear that there is only one temperature, 1675.6 K, at which a least squares linear regression line of log γ vs ionic radius for Gd, Tb, Dy, Ho, Er and Lu will intersect $\gamma_{Sm} = 1$ in Fig. 3. At all other temperatures, there must be a sharp change in γ between Gd and Sm. These conclusions hold no matter what value is assumed for

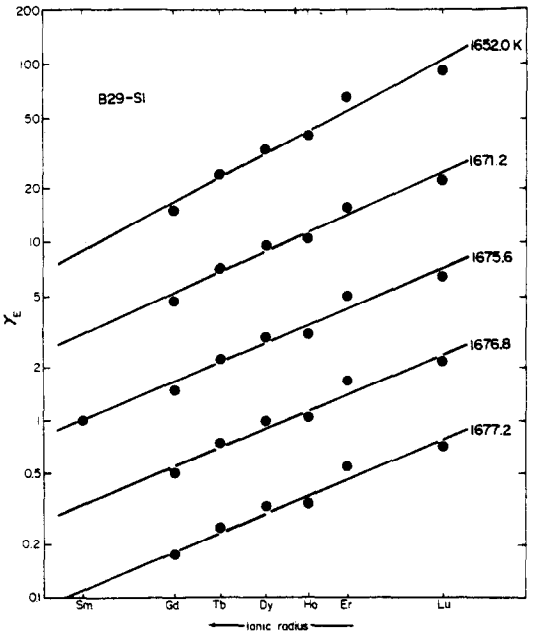

Fig. 3. There is only one perovskite removal temperature at which a linear regression through Gd, Tb, Dy, Ho, Er and Lu points on a log γ vs ionic radius plot intersects $\gamma_{Sm} = 1$. At all other temperatures, there would have to be a discontinuous jump in activity coefficient between Sm and Gd. REE substitute into the 12-coordinated Ca site in perovskite. Since ionic radii are not available for this coordination number, we have used the 8-coordinated ionic radii of SHANNON (1976) in all figures, but have not written them on the x-axes.

γ_{Sm}. Similarly, there must be unique temperatures at which heavy REE regression lines intersect $\gamma_{Nd} = 1$ or $\gamma_{Gd} = 1$.

It may not seem fair to use thermodynamic data adjusted to fit an ideal solution model for B-32W to model non-ideal solution. However, examination of Table 2 reveals that the adjustments made to the free energies for Gd, Tb, Dy, Er and Lu are small (< 1 kcal). Only Ho required a large adjustment. If the latter adjustment had not been made, all models would have consistently overestimated the enrichment factor for Ho.

Method of calculation. We calculated the perovskite removal temperature at which the heavy REE regression line of log γ vs ionic radius intersects $\gamma_{Sm} = 1$ for all group II inclusions for which data are available for two or more REE of the group Gd, Tb, Dy, Ho, Er and Lu. This was done by computing an F_{gas}^{E}/F_{gas}^{Sm} value for each heavy REE in the above group from their observed enrichment factors, J^E's, and the enrichment factor for Sm, J^{Sm}:

$$\frac{F_{gas}^{E}}{F_{gas}^{Sm}} = \frac{J^{E}}{J^{Sm}}. \qquad (17)$$

A temperature was selected and γ_E's were calculated from (11) and (12), using the ratio computed in (17). The log γ vs ionic radius regression coefficients were then calculated and, from these, γ at the ionic radius of Sm. This series of calculations was repeated at different temperatures until the temperature at which the regression line passed

Table 3. Results of REE condensation models of all inclusions for which two or more of the REE Gd, Tb, Dy, Ho, Er and Lu have been analyzed

Sample	One-component, non-ideal solution model		Two-component, ideal solution model				REE used in models						
	T_{per} (K)	γ_{Lu}/γ_{Sm}	T_{per} (K)	F_1	F_2	J_1	Gd	Tb	Dy	Ho	Er	Lu	Ref.
FG-13	1676.9	2.88	1677.2	0.985	0.015	57.4		×	×			×	1,2
A-19	1673.9	148	1677.0	0.844	0.156	13.0		×	×		×	×	3
CG-5	1675.3	21.3	1676.9	0.760	0.240	82.5		×	×			×	4,5
B29-S1	1675.6	7.22	1676.7	0.971	0.029	29.5	×	×	×	×	×	×	6
B-32W	1676.5	1.00	1676.5	1.000	0.000	59.1	×	×	×	×	×	×	6
A-10	1676.4	1.28	1676.1	0.987	0.013	32.5	×	×	×	×	×	×	3
37	1674.9	18.8	1676.1	0.853	0.147	18.2	×	×	×	×			7
A-21	1669.7	57.2	1675.8	0.927	0.073	23.7		×	×			×	3
G_p	1672.8	5.34	1675.7	0.994	0.006	26.0	×		×		×	×	8
4691	1672.1	16.6	1675.0	0.890	0.110	43.0	×	×	×	×	×		7
G_w	1667.6	78.6	1674.7	0.936	0.064	15.8	×		×		×	×	8
13	1665.3	46.9	1674.5	0.953	0.047	28.8		×				×	9
4692	1671.2	8.46	1674.3	0.948	0.052	37.4	×	×	×	×	×		7
3598	1666.6	32.7	1673.6	0.938	0.062	21.7	×	×	×	×	×		7
3643	1662	712	1673.2	0.699	0.301	18.4	×	×	×	×	×		7
3803	1658	92.2	1672.0	0.948	0.052	14.1	×	×	×	×	×		7
CG-12	1540	2093	1671.7	0.920	0.080	24.1			×			×	2
15	1639	151	1670.9	0.961	0.039	23.7		×				×	9
I-3	1630	138	1667.7	0.966	0.034	23.6	×	×	×	×	×	×	6
A-2	1649	1235	1664.0	0.764	0.236	12.4	×	×	×	×	×	×	6

References: 1, GROSSMAN and GANAPATHY (1976b); 2, Unpublished data from this laboratory; 3, PALME (personal communication); 4, GROSSMAN and GANAPATHY (1976a); 5, GROSSMAN *et al.* (1977); 6, CONARD (1976); 7, MASON and MARTIN (1977); 8, TANAKA and MASUDA (1973); 9, NAGASAWA *et al.* (1977).

through $\gamma_{Sm} = 1$ was found. The computations were done at 0.1° intervals from 1677.4 to 1664 K, 1° intervals from 1664 to 1636 K, 10° intervals from 1630 to 1600 K and 20° intervals below 1600 K. Once the correct temperature was found, activity coefficients for heavy REE were calculated from the regression coefficients and used with F_{gas} to calculate model REE enrichment factors. γ_{Lu}/γ_{Sm} was also calculated for use as an indicator of the steepness of the activity coefficient vs ionic radius relationship. The results of these calculations are given in Table 3 and calculated REE patterns are compared with actual REE patterns in Figs 4–8. Given in Table 4 are the mean deviations of theoretical from observed REE patterns, which are useful as a measure of goodness of fit. This value was calculated for each inclusion from:

$$\text{M.D.} = \frac{1}{n}\sum_{i=1}^{n}\frac{|J^i_{calc} - J^i_{samp}|}{J^i_{samp}} \times 100, \qquad (18)$$

where J^i_{calc} and J^i_{samp} are, respectively, calculated and observed enrichment factors for REE i and n is the number of REE analyzed from the group Gd, Tb, Dy, Ho, Er and Lu. When only two of the latter REE have been measured in an inclusion, M.D. is zero for that inclusion, because the regression line will pass through both points. Also given in Table 4 is the deviation between observed and calculated enrichment factors for Tm. When no Tm analysis was given, Tm was assumed to have the same enrichment factor as Sm. The non-ideal solid solution model provides reasonably good fits to the group II REE patterns, with a mean deviation of 11.4% averaged over the 17 inclusions with analyses of three or more heavy REE, and fits Tm well when inclusions give high γ_{Lu}/γ_{Sm} values.

Models with non-ideal solution of Sm. We have also investigated models in which γ_{Sm} has values ranging from 0.01 to 1000. As γ_{Sm} increases from unity, calculated perovskite removal temperatures drop, as can be seen in Fig. 3, and the range of perovskite removal temperatures becomes wider in order to accommodate all inclusions. As γ_{Sm} drops below 1, calculated perovskite removal temperatures rise, and if $\gamma_{Sm} = 0.01$, all inclusions have perovskite removal temperatures within 1° of 1677.4 K. The order of inclusions with decreasing perovskite removal temperature and increasing γ_{Lu}/γ_{Sm} ratio is independent of the value of γ_{Sm} in models where the latter is constant. This order also remains the same in models in which γ_{Sm} or log γ_{Sm} increases or decreases linearly with temperature. The goodness of fit to observed REE enrichment factors does not change significantly when values other than unity are used for γ_{Sm}.

Alternative γ vs ionic radius functions. In the previous discussion, we used a linear log γ vs r function to model the variation of activity coefficient with ionic radius. Other functions describing this relationship can also be used. Upon examination of Fig. 3, it is seen that if we use a function that is fairly straight through the heavy REE and then curves sharply downward through $\gamma_{Sm} = 1$, lower perovskite removal temperatures will be obtained. The difficulty with this type of function comes when it is extrapolated to the light REE, where the predicted γ's will be so low that the light REE, especially La and Ce, will condense significantly prior to perovskite removal and severe fractionations in the light REE patterns of group II inclusions will occur. If we use a function that is fairly linear through the heavy REE and curves sharply upward through $\gamma_{Sm} = 1$, higher perovskite removal temperatures will be obtained. Finally, the log γ vs r function provides superior fits to group II inclusions than do the other functions tested.

Temperature variation of γ_{Lu}/γ_{Sm}. Although the one-component, non-ideal solid solution model is capable of fitting the REE patterns of group II inclusions fairly well, it requires that the relationship between log γ and ionic radius change rapidly with falling temperature. Shown in Fig. 9 is a plot of γ_{Lu}/γ_{Sm} vs perovskite removal temperature assuming $\gamma_{Sm} = 1$. *γ_{Lu}/γ_{Sm} increases rapidly and irregularly with falling temperature. The increase is by a factor of about 400*

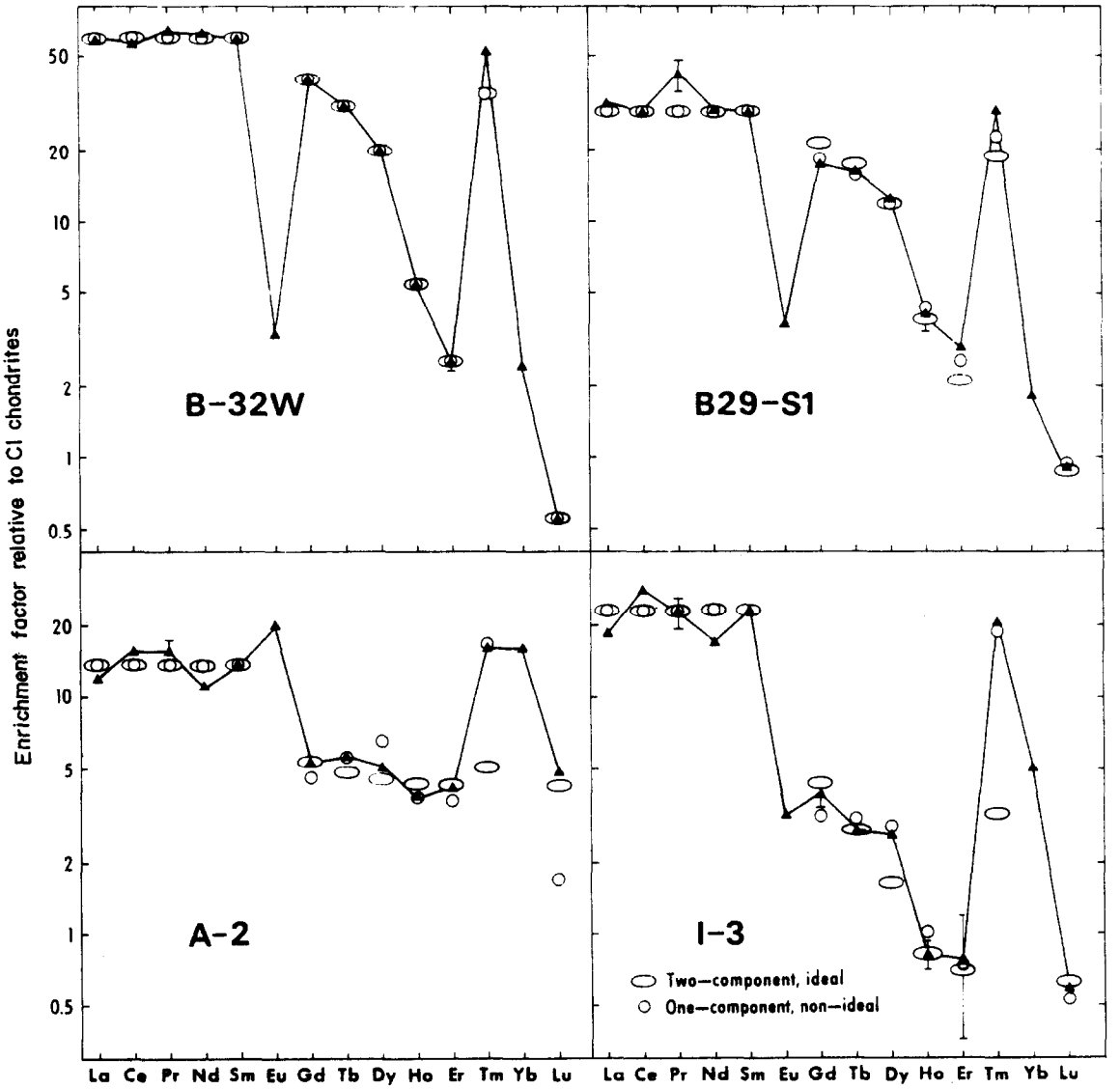

Fig. 4. Observed REE patterns are compared here with those calculated by the one-component, non-ideal and two-component, ideal solution models. REE abundances in fine-grained inclusions B29-S1, B-32W and I-3 and coarse-grained inclusion A-2 were determined by RNAA by CONARD (1976).

over a 20° temperature range, but inclusions with virtually the same perovskite removal temperature can have γ_{Lu}/γ_{Sm} values differing by as much as a factor of 30. When the calculations are repeated for $\gamma_{Sm} = 100$, γ_{Lu}/γ_{Sm} increases by a factor of about 800 over a 100° temperature range. If $\gamma_{Sm} = 0.1$, γ_{Lu}/γ_{Sm} increases by a factor of 400 over a 6° temperature range. REE partitioning experiments between perovskite and liquid (RINGWOOD, 1975; NAGASAWA *et al.*, 1976) show that perovskite has a strong affinity for REE, so that if REE solid solution in perovskite departs from ideality under solar nebular condensation conditions, activity coefficients are probably less than unity. Thus, if $\gamma_{Sm} \neq 1$, the range of perovskite removal temperatures which the inclusions have experienced would probably have been smaller than that indicated in Fig. 9.

While both absolute activity coefficients and activity coefficient ratios for REE in perovskite could vary with temperature, the extreme variations in the activity coefficient ratio of two elements, Sm and Lu, (whose ionic radii differ by only 9%), over a 20° or even a 100° temperature range seem very unlikely, especially at the high temperatures under consideration. The BOYNTON (1975) model thus fails its second test, since unreasonably large variations in relative activity coefficients are required over a narrow temperature range.

Non-ideal solid solution of REE in perovskite. BOYNTON (1975) found that in order to fit inclusion G_p of TANAKA and MASUDA (1973), the REE host phase must strongly favor light over heavy REE. We have now shown that, when modelled with a BOYNTON (1975) type model, some inclusions require the host phase for REE to have an even stronger preference for light over heavy REE than was called for by BOYNTON (1975). Boynton considered several candidates for this

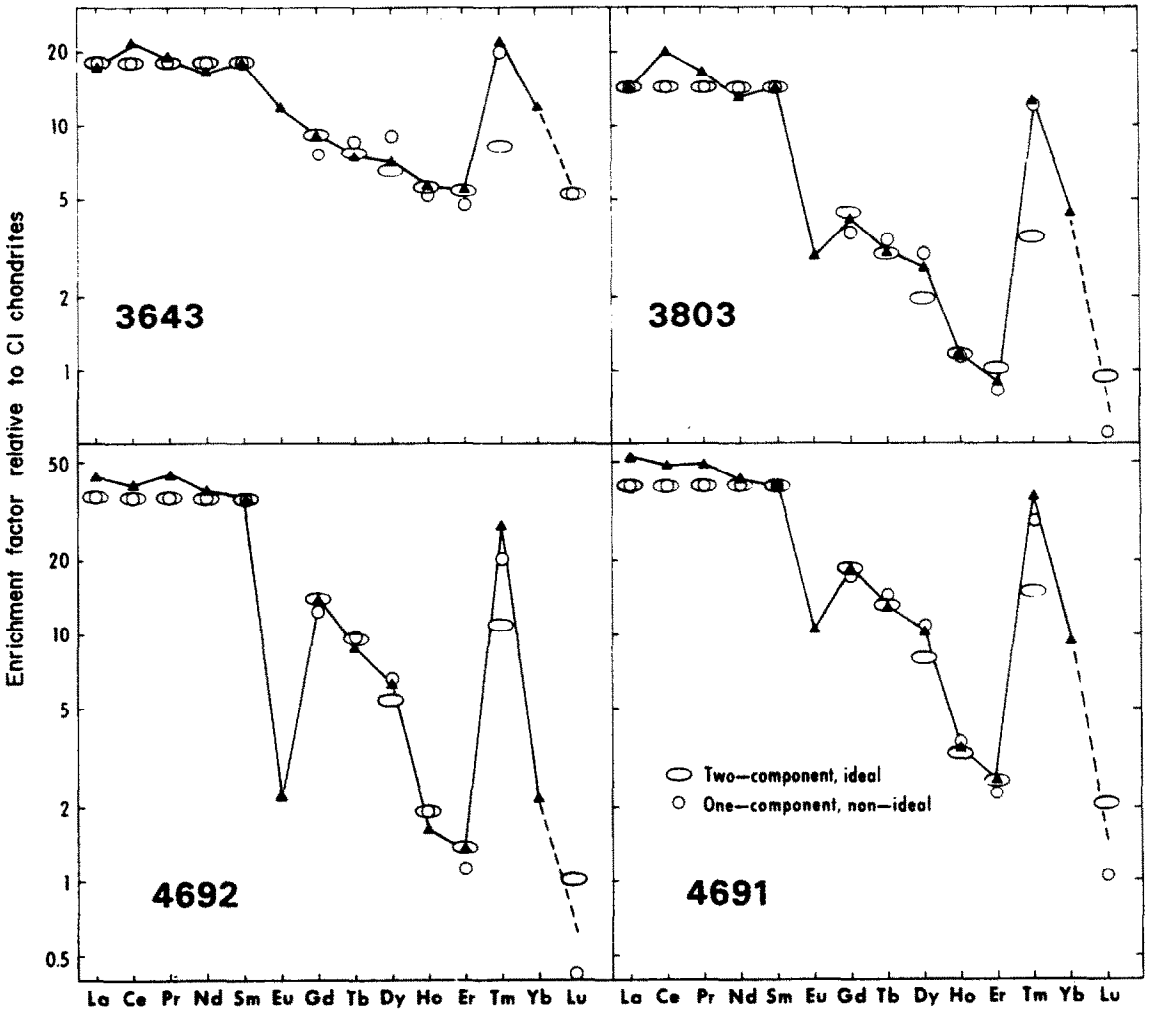

Fig. 5. Same as Fig. 4. When a measurement of an individual REE other than Tm was missing, the REE pattern was drawn through the mean enrichment factor calculated by the two REE condensation models. REE abundances in fine-grained inclusions 3643, 3803 and 4692 and coarse-grained inclusion 4691 were determined by SSMS by MASON and MARTIN (1977).

host phase. Hibonite was considered as a possibility but there was no information on the ability of REE to substitute into its structure. Yttrium sesquioxide was eliminated because it should have an activity coefficient minimum at the ionic radius of Y^{3+}, which is between those of Dy^{3+} and Ho^{3+}. Boynton concluded that the host phase was most likely to be perovskite on the basis of the highly fractionated, light REE-enriched REE patterns of terrestrial perovskites found by BORODIN and BARINSKII (1960). We must now consider whether the highly non-ideal solid solution behavior of REE in perovskite required by the one-component model is reasonable.

There is no unequivocal evidence from either analyses of natural perovskites or experimental partitioning experiments that perovskite preferentially incorporates light over heavy REE. BORODIN and BARINSKII (1960) measured REE abundances in perovskites from various rock types and found perovskite to be strongly enriched in light over heavy REE. These data cannot be used as evidence in favor of non-ideal solid solution of REE in perovskite because Borodin and Barinskii analyzed neither coexisting minerals nor bulk host rocks. Furthermore, the Borodin and Barinskii perovskites contain 2.4–11.3 wt% total REE, so that their crystal structures may be sufficiently different from those of perovskites in which REE are minor or trace constituents that Henry's Law is no longer obeyed. Experimental measurements of REE partitioning between perovskite and liquid have been made in natural (Onuma, Ninomiya, Blanchard and Nagasawa, quoted in NAGASAWA *et al.*, 1976) and synthetic (RINGWOOD, 1975; NAGASAWA *et al.*, 1976) systems. Assuming ideal solution behavior of REE in all three liquids, γ_{Lu}/γ_{Sm} values of 5, 7 and 18 for solid solution of REE in perovskite are obtained for the experiments of ONUMA *et al.*, NAGASAWA *et al.* and RINGWOOD, respectively. Of the 20 inclusions modelled in Figs 4–8, 5 require γ_{Lu}/γ_{Sm} values less than or equal to 5, 10 require γ_{Lu}/γ_{Sm} values less than or equal to 20 and 10 require γ_{Lu}/γ_{Sm} values from 33 to 2090. Thus, experimental measurements from

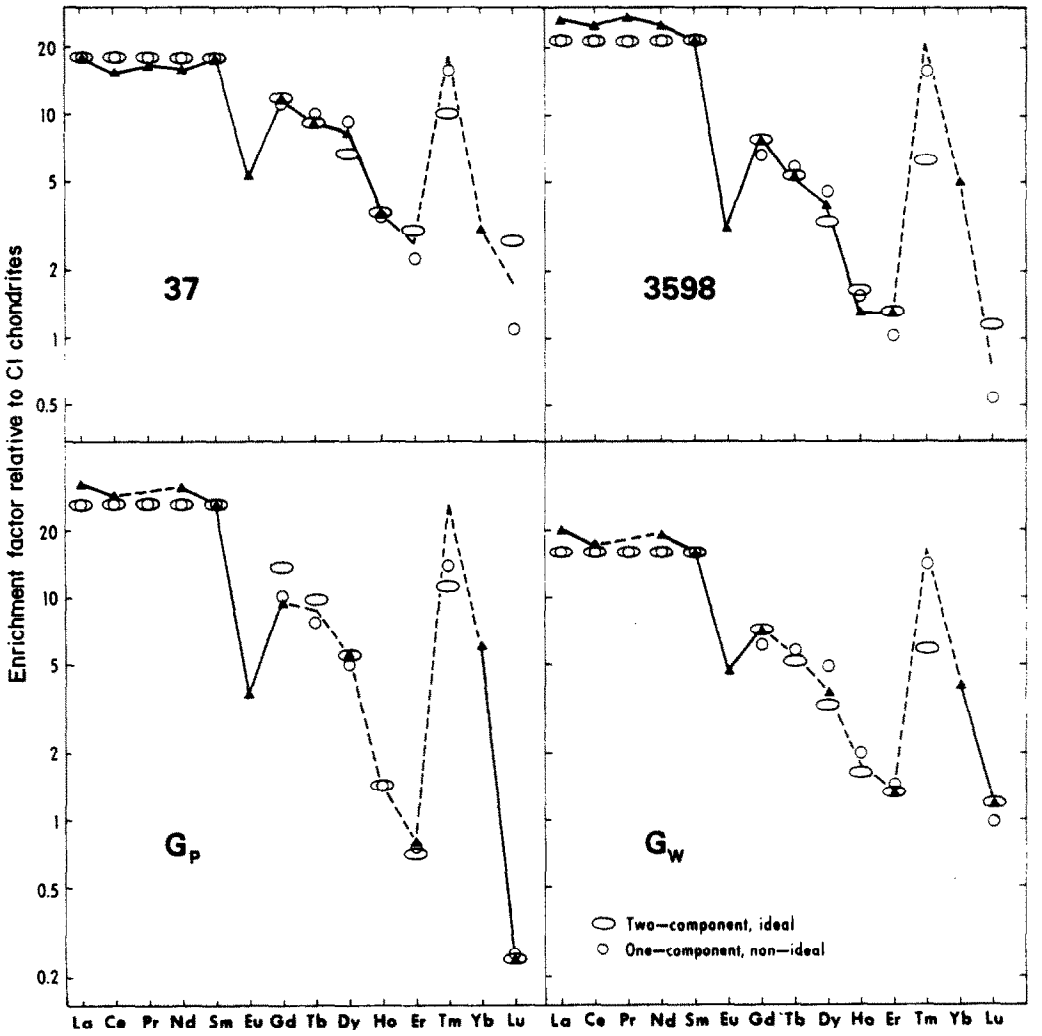

Fig. 6. Same as Fig. 5. Since Tm was not analyzed in any of these inclusions, REE patterns were drawn such that Tm has the same enrichment factor as Sm. REE abundances were determined in fine-grained inclusions 37 and 3598 by SSMS by MASON and MARTIN (1977) and in fine-grained inclusions G_p and G_w by MSID by TANAKA and MASUDA (1973).

which approximate activity coefficients can be estimated do not permit the γ_{Lu}/γ_{Sm} values required by the one component, non-ideal solid solution model for many inclusions. Furthermore, REE partitioning between perovskite and liquid may not be applicable to solar nebular condensation because of differences in minor and trace element content of the perovskites.

The crystal structure of perovskite is quite versatile, as demonstrated by the hundreds of perovskite structure compounds listed by GOODENOUGH and LONGO (1970). There exist several perovskite structure compounds, $LnScO_3$, $LnVO_3$, $LnTiO_3$ and $LnAlO_3$, which are isostructural with and have similar lattice dimensions to $CaTiO_3$. The minor elements Al, Sc and V are known to be present in perovskite from Allende coarse-grained inclusions (GROSSMAN, 1975; ALLEN *et al.*, 1978). Since perovskite condensation from a solar nebular gas occurs under highly reducing conditions, small amounts of Ti^{3+} may be present in condensate perovskite. The possibility of large differences in activity coefficients between Sm and Lu seems remote when there are cations present in perovskite which can couple with lanthanides in substitution in $CaTiO_3$ to give unit cell volumes larger than (by 8–16% for $LnScO_3$), smaller than (by 7–12% for $LnAlO_3$) and nearly the same size as (within 4% for $LnTi^{3+}O_3$ and $LnVO_3$) $CaTiO_3$. Furthermore, the change in unit cell volumes from $SmTiO_3$ to $LuTiO_3$ and $SmAlO_3$ to $LuAlO_3$ are only 3 and 4%, respectively, certainly not enough to produce γ_{Lu}/γ_{Sm} values as high as 2000.

The one-component, non-ideal solid solution model is seen to require large changes in activity coefficient vs ionic radius relationships for REE in perovskite over a small range of temperature. These changes are not a smooth function of temperature. Although they may not be applicable to the conditions under consideration, experimental measurements of partition coefficients do not support γ_{Lu}/γ_{Sm} values greater than ~20, while the model requires this ratio to be greater than 20 for 10 of the 20 group II inclusions for which REE patterns have been determined.

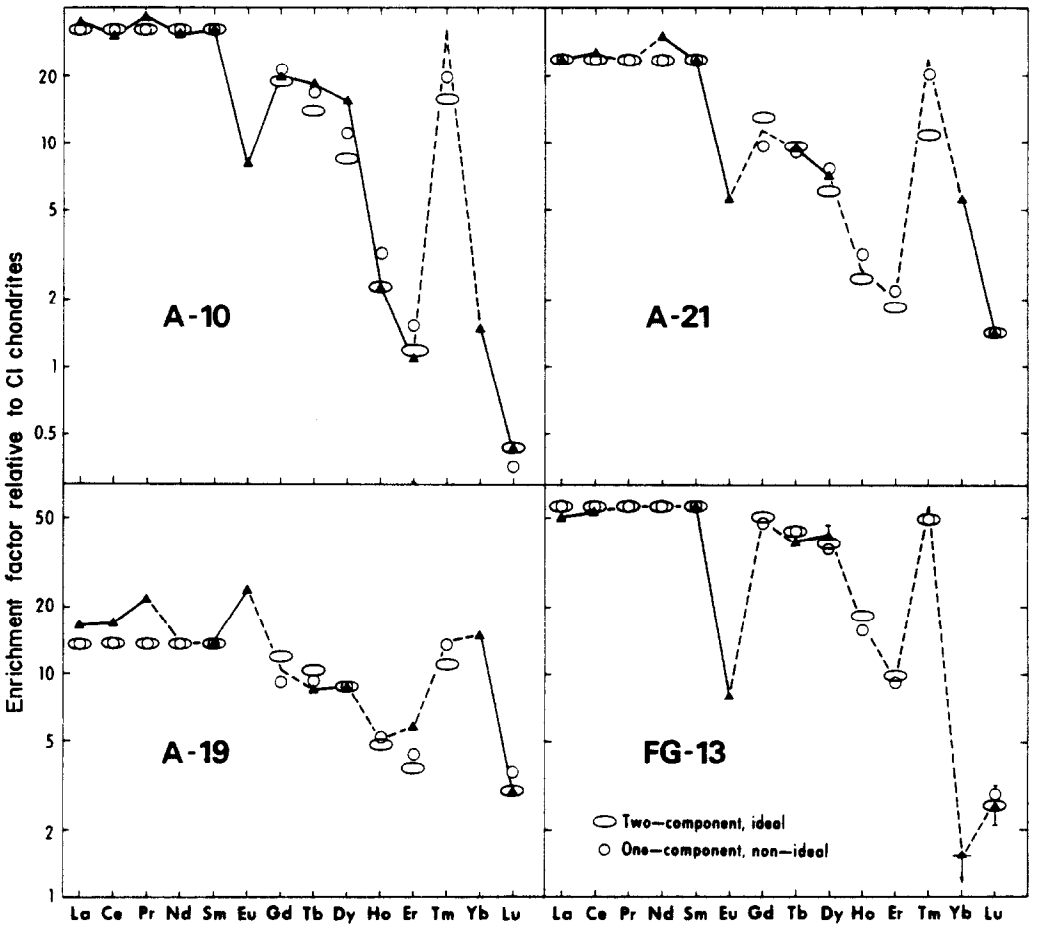

Fig. 7. Same as Fig. 6. REE abundances in fine-grained inclusions A-10 and A-19 were determined by RNAA by PALME (personal communication) and in fine-grained inclusions A-21 (PALME, personal communication) and FG-13 (GROSSMAN and GANAPATHY, 1976b and unpublished data from this laboratory) by INAA.

Two-component, ideal solution model

As seen in the previous section, the assumption that the gas remaining after perovskite removal is the only REE-bearing component in group II inclusions requires that thermodynamic quantities (specifically, activity coefficients) must vary by unreasonable amounts from inclusion to inclusion. We now propose what we believe to be a more plausible model. One set of thermodynamic data must be used to model all inclusions, so that, in addition to temperature, some other parameter must vary among inclusions in order to explain the details of each heavy REE pattern. TANAKA and MASUDA (1973) noted that the REE pattern of G_w, which was removed from the same inclusion as sample G_p (B. MASON, personal communication), could be explained by mixing of the REE pattern of G_p with a chondritic REE pattern. We found that addition to the group II inclusions of a second REE-bearing component with uniform enrichments of all REE will adequately explain the observed REE patterns in all group II inclusions. This second component carries 0–30% of the total Sm in the inclusions. As shown later, some inclusions with a large fraction of their Sm in this second component require this component to have Sm enrichment factors greater than that of Allende matrix or bulk Allende. We have therefore chosen the second component such that it has all 14 REE enriched relative to Cl chondrites by the mean enrichment factor for all REE in the 17 group I coarse-grained inclusions analyzed by CONARD (1976), GROSSMAN and GANAPATHY (1976a), GROSSMAN *et al.* (1977) and DAVIS *et al.* (1978a, b), 17.8.

Method of calculation. For each group II inclusion, the weight fraction of this second component needed to minimize the mean deviation (18) of calculated from observed enrichment factors for all REE analyzed from the group Gd, Tb, Dy, Ho, Er and Lu was calculated in the following way. For each REE,

$$J^E = F_1 J_1^E + F_2 J_2^E, \tag{19}$$

where F_1 and F_2 are the weight fractions of component 1 (the gas remaining after perovskite removal, condensed into solid material) and component 2 (which has a flat REE pattern), respectively, and J^E, J_1^E and J_2^E are REE enrichment factors relative to Cl chondrites in the bulk

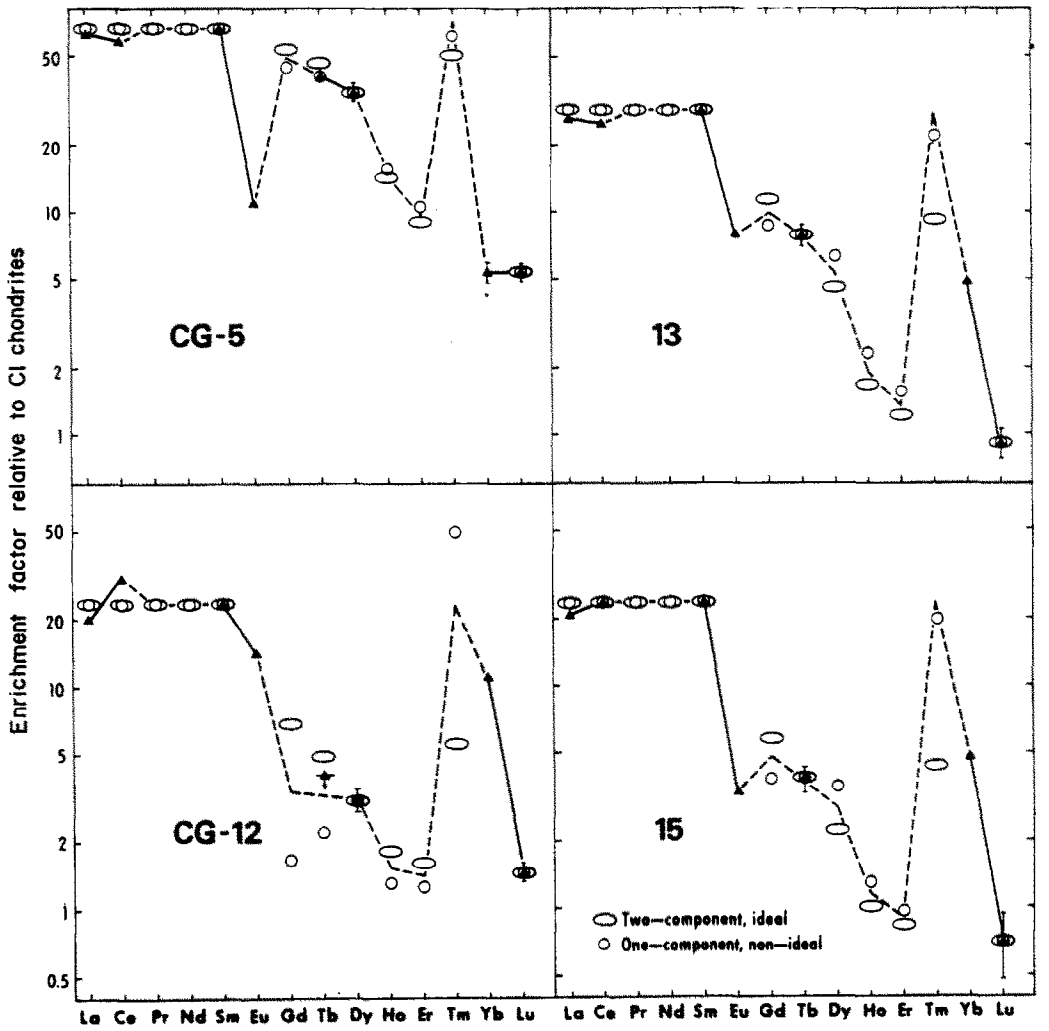

Fig. 8. Same as Fig. 6. REE abundances in coarse-grained inclusions CG-5 (GROSSMAN and GANAPATHY, 1976a; GROSSMAN *et al.*, 1977) and CG-12 (unpublished data from this laboratory) and fine-grained inclusions 13 and 15 (NAGASAWA *et al.*, 1977) were determined by INAA.

inclusion, component 1 and component 2, respectively. We have assigned component 2 the mean enrichment factor of all REE in group I inclusions, so

$$J_2^E = 17.8. \tag{20}$$

Substituting (20) into (19) and writing (19) for Sm,

$$J^{Sm} = F_1 J_1^{Sm} + 17.8F_2. \tag{21}$$

Using the observed value of J^{Sm} in the sample, J^{Sm}_{samp}, and solving (21) for J_1^{Sm}, we find that

$$J_1^{Sm} = \frac{J^{Sm}_{samp} - 17.8F_2}{F_1}. \tag{22}$$

For each REE at a given perovskite removal temperature, the enrichment factor in component 1 can be calculated from F^E_{gas}, F^{Sm}_{gas} and J_1^{Sm}:

$$J_1^E = \frac{F^E_{gas}}{F^{Sm}_{gas}} J_1^{Sm}. \tag{23}$$

Substituting (22) into (23), we find that

$$J_1^E = \frac{F^E_{gas}}{F^{Sm}_{gas}}\left(\frac{J^{Sm}_{samp} - 17.8F_2}{F_1}\right) \tag{24}$$

and substituting (24) into (19), and cancelling the F_1's

$$J^E = \frac{F^E_{gas}}{F^{Sm}_{gas}}(J^{Sm}_{samp} - 17.8F_2) + 17.8F_2. \tag{25}$$

For each value of F_2 at a given perovskite removal temperature, J^E's can be calculated for each REE in any inclusion. The mean deviation of calculated from observed J^E's can be computed for Gd, Tb, Dy, Ho, Er and Lu within any inclusion using (18). Plots of M.D. vs F_2 show that there is a single minimum value of M.D. for a given perovskite removal temperature, and that at the value of F_2 at which the minimum M.D. occurs, calculated and observed J^E's will be equal for one of the group Gd, Tb, Dy, Ho, Er and Lu. Calculator programs to find the value of F_2 at which M.D. is minimized are quite time consuming. Thus, M.D. was calculated only at the values of F_2 where observed and calculated J^E's matched for each element in the above group, permitting us to find the value

Table 4. Comparison of fits to Tm and to analyzed REE from the group Gd, Tb, Dy, Ho, Er and Lu. The samples are the same as those in Table 3

Sample	One-component, non-ideal solution model		Two-component, ideal solution model	
	M.D.	D.Tm†	M.D.	D.Tm†
FG-13	11.9	−12.9*	8.8	−13.4*
A-19	14.2	−1.0*	15.3	−19.1*
CG-5	1.0	−10.0*	5.3	−26.4*
B29-S1	10.2	−23.1	11.0	−36.8
B-32W	0	−34.1	0	−34.1
A-10	22.8	−38.6*	14.4	−50.6*
37	4.6	−12.8*	5.3	−43.6*
A-21	4.8	−12.1*	5.1	−52.8*
G_p	6.0	−46.4*	13.6	−57.2*
4691	8.5	−18.9	5.1	−58.4
G_w	19.7	−11.0*	4.3	−63.2*
13		−21.6*		−67.5*
4692	13.4	−25.9	8.1	−59.6
3598	17.1	−26.7*	8.8	−71.1*
3643	16.2	−9.2	2.3	−62.0
3803	10.3	−4.7	8.9	−72.7
CG-12		+109.6*		−76.8*
15		−14.0*		−81.2*
I-3	12.6	−9.9	10.8	−84.3
A-2	20.6	+5.0	8.2	−68.9
	Avg 11.4 ± 1.6%		Avg 8.0 ± 1.0%	

† $\text{D.Tm} = \left(\frac{J^{\text{Tm}}_{\text{calc}} - J^{\text{Tm}}_{\text{samp}}}{J^{\text{Tm}}_{\text{samp}}}\right) \times 100.$

* No Tm data available; Tm enrichment factor assumed to be equal to that of Sm.

of F_2 which gave the minimum M.D. Values of F_2 were calculated from the following expression, which is obtained by solving (25) for F_2:

$$F_2 = \frac{J^{\text{E}} - \frac{F^{\text{E}}_{\text{gas}}}{F^{\text{Sm}}_{\text{gas}}} J^{\text{Sm}}_{\text{samp}}}{17.8\left(1 - \frac{F^{\text{E}}_{\text{gas}}}{F^{\text{Sm}}_{\text{gas}}}\right)}. \quad (26)$$

This calculation was repeated at 0.1° intervals of perovskite removal temperature. The temperature which gave the lowest M.D. was adopted as the model perovskite removal temperature and model J^{E} values were calculated from (25), using the value of F_2 that gave the minimum M.D. Values for perovskite removal temperature, F_1, F_2 and J^{Sm}_1 for each inclusion are given in Table 3. The M.D. values obtained from the two-component, ideal-solution model are compared with those of the one-component, non-ideal solution model in Table 4. Also compared are deviations of calculated from observed enrichment factors for Tm, calculated from the two models. Model enrichment factors for each inclusion are plotted in Figs 4–8. The inclusions contain from 0 to 30.1 wt% of component 2. Perovskite removal temperatures range from 1664.0 to 1677.0 K, only 0.4° below the temperature at which perovskite first appears.

There is another possible refractory mineral host for the REE, hibonite. Corundum is the most refractory major mineral predicted to condense from a gas of solar composition. Because hibonite ($CaAl_{12}O_{19}$) is found in Allende and corundum is not, hibonite is thought to have condensed instead of corundum (GROSSMAN, 1972). Unfortunately, no thermodynamic data are available for hibonite, so that its condensation behavior cannot be calculated in detail. In the case of hibonite condensation, we can say, however, that Ca sites would have become available for REE substitution at a higher temperature than the perovskite condensation temperature. This would have the effect of slightly increasing the removal temperatures relative to those calculated for perovskite.

Alternative enrichment factors for component 2. Values of J_2 other than 17.8 can be used in two-component models, but, for each inclusion, there is a lower limit to this enrichment factor. This lower limit can be calculated by application of the following useful property of the two-component model: the amounts of any rare earth element in components 1 and 2 are constants (L_1 and L_2) and are equal to the products of weight fractions (F_1 and F_2) and enrichment factors (J_1 and J_2) for each component,

$$L_1 = F_1 J_1 \text{ and } L_2 = F_2 J_2. \quad (27)$$

The lower limit to J_2 for each inclusion can be found by calculating L_2 for any REE using the model value of F_2 and $J_2 = 17.8$ and then calculating J_2 for $F_2 = 1$. The minimum enrichment factor for component 2 in group II inclusions with non-zero amounts of this component ranges from 0.11 to 5.36, relative to Cl chondrites. The minimum enrichment factor for component 2 is higher than the enrichment factor of bulk Allende, 2.0, in 4 out of 20 inclusions

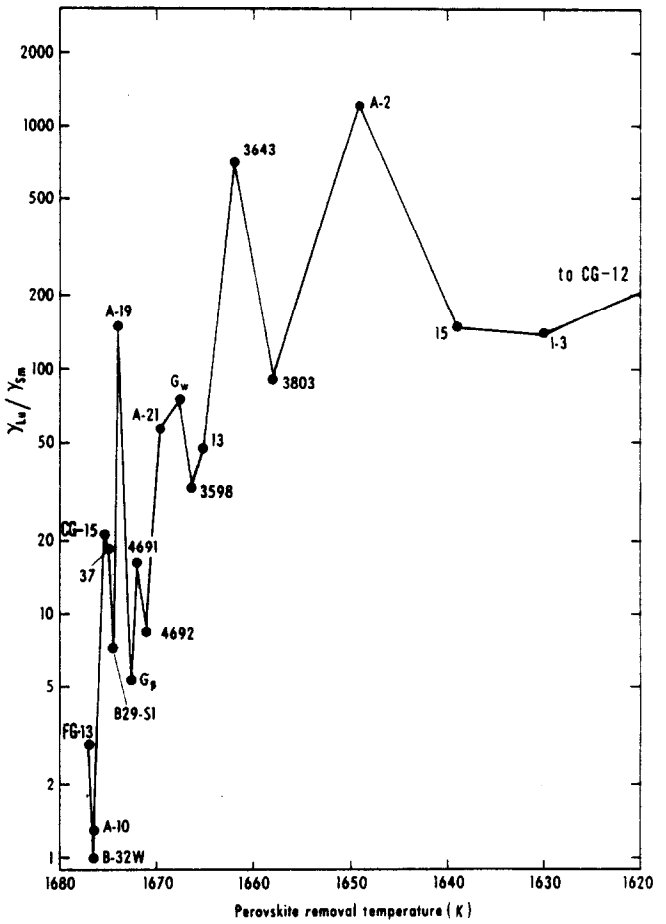

Fig. 9. In the one-component, non-ideal solution model with $\gamma_{Sm} = 1$ at all temperatures, γ_{Lu}/γ_{Sm}, which is calculated from the slope of the log γ vs ionic radius function, must rise sharply and irregularly with decreasing perovskite removal temperature. This drastic change in the solid solution behavior of the REE host mineral over a narrow temperature range provides the strongest evidence against one-component REE condensation models.

modelled, so that component 2 cannot be identified with matrix contamination in at least these 4 inclusions. We will return to the problem of the identity of component 2 later.

A consequence of models with large fractions of component 2 is that as F_2 approaches 1, F_1 becomes very small and enrichment factors in component 1 become very large. This means that component 1 could be a trace mineral that contains REE as major constituents and has a fractionated REE pattern. A trace mineral host for the REE is permitted by the existing analyses of mineral separates of a group II inclusion by NAGASAWA *et al.* (1977), since such a phase may be a contaminant in all density fractions.

Other refractory elements in component 2. If the gas from which group II inclusions condensed experienced removal of perovskite, elements more refractory than perovskite should also have been removed and the concentrations of these elements in group II inclusions should be controlled by the amount of component 2. Zr, Hf, Ir and Re are the only elements more refractory than perovskite that have been analyzed in group II inclusions. All of these elements are strongly depleted in group II inclusions, but insufficient data exist for all but two of them, Zr and Ir, to search for relationships between refractory trace element abundances and the fraction of component 2. Plotted in Fig. 10 is the Zr content of group II inclusions vs the Sm content calculated to be due to component 2. If the enrichment factor relative to Cl chondrites for Zr in component 2 is the same as that for REE, the inclusions should lie along a line whose slope equals the Zr/Sm ratio in Cl chondrites and whose intercept is at the origin. Examination of Fig. 10 shows that all group II inclusions for which data exist plot near this reference line, so that Zr and REE are enriched to the same degree in component 2. GROSSMAN *et al.* (1977) found that Zr and REE are equally enriched relative to Cl chondrites in both individual and the mean of all coarse-grained inclusions. Plotted in Fig. 11 is the Ir content of group II inclusions vs the Sm content due to component 2. If the enrichment factor for Ir in component 2 is the same as that for REE, the inclusions should

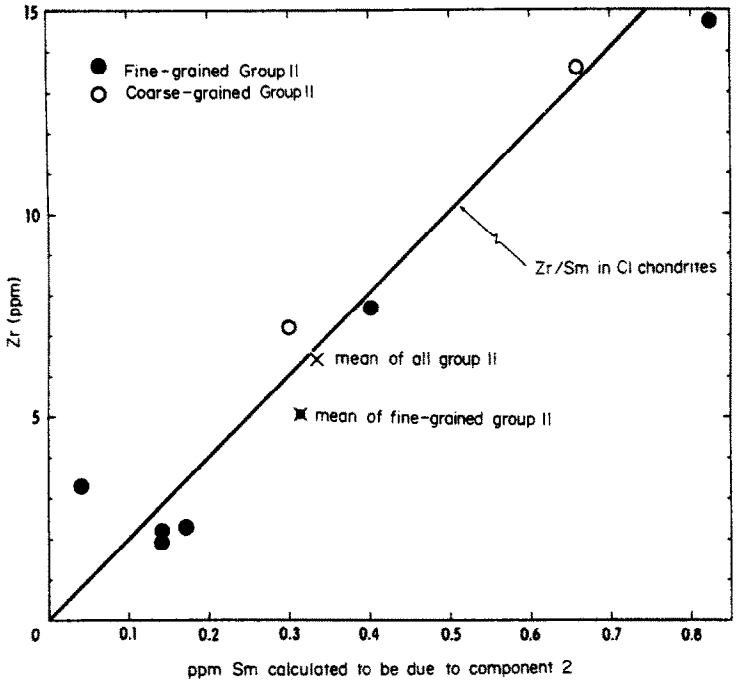

Fig. 10. Zr and Sm are enriched by the same amount relative to Cl chondrites in component 2. The Zr content of Cl chondrites was taken from GANAPATHY *et al.* (1976).

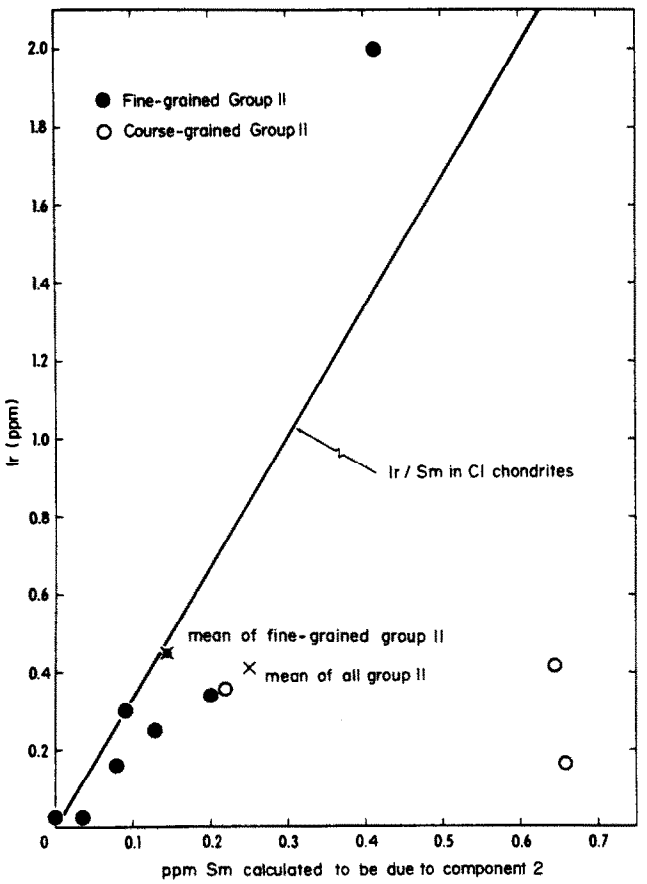

Fig. 11. Ir and Sm are both enriched, but by variable amounts relative to Cl chondrites, in component 2. The Ir content of Cl chondrites was taken from KRÄHENBÜHL *et al.* (1973).

lie along a line whose slope equals the Cl Ir/Sm ratio and whose intercept is at the origin. Examination of Fig. 11 shows that many fine-grained group II inclusions lie near the reference line, but two coarse-grained group II inclusions lie far from the line, on the low Ir side. It is noted, however, that the mean Ir and Sm contents of these inclusions plot very close to the line, particularly when the coarse-grained group II inclusions are ignored. This is again reminiscent of the behavior of these two elements in coarse-grained inclusions in which GROSSMAN *et al.* (1977) found that Ir and Sm are often highly fractionated from one another relative to Cl chondrites, even though they are unfractionated in the mean of all such inclusions. On the average, component 2 is thus seen to be uniformly enriched in REE, Zr and Ir. There are only two known types of objects in Allende which have this characteristic: coarse-grained inclusions (GROSSMAN and GANAPATHY, 1976a; GROSSMAN *et al.*, 1977) and amoeboid olivine aggregates (GROSSMAN *et al.*, 1979). Since olivine has not been reported in any group II inclusion, coarse-grained inclusions remain as the only recognized candidate for component 2.

Two-component, ideal solution model with unadjusted thermodynamic data. We have used thermodynamic data adjusted to fit B-32W to model group II inclusions in this section. Examination of Table 2 shows that the adjustments made to ΔG's for Gd, Tb, Dy, Er and Lu are very small and that only for Ho were significant adjustments made. Had we used unfitted thermodynamic data to model group II inclusions, the perovskite removal temperatures would have been nearly the same and the M.D. values would have been somewhat larger because we would have consistently over-estimated the enrichment factor for Ho. Thus, although adjustment of thermodynamic data improves the fit of the two-component, ideal solution model, it is not essential to its success.

Two-component, non-ideal solution models

Non-ideal solid solution of REE in perovskite is permissible if the relationship between activity coefficient and ionic radius does not change drastically with temperature. We have investigated one such two-component model in which the ionic radius vs activity coefficient relationship is invariant with temperature, activity coefficients of the light REE are unity and log γ increases linearly with ionic radius from Sm to Lu. In order to model Tm in B-32W as closely as possible while retaining a linear relationship between log γ and ionic radius, γ_{Ho} and γ_{Lu} must be as high as possible. This situation is achieved by adjusting ΔG_1 and ΔG_2 for Ho and Lu so that they are as refractory as possible within the error bounds derived previously. Using these newly-adjusted ΔG_1 and ΔG_2 values for Ho and Lu, we determined the temperature at which the log γ vs ionic radius regression line through the γ_{Ho} and γ_{Lu} values required to fit B-32W passed through $\gamma_{Sm} = 1$, 1672.0 K, by a trial and error method similar to that used in the one-component, non-ideal solution model. In this particular model, $\gamma_{Lu}/\gamma_{Sm} = 16.9$, a value that would be compatible with perovskite-liquid partition experiments if $\gamma_{Lu}/\gamma_{Sm} = 1$ in the liquids employed. We then calculated γ's for Gd, Tb, Dy, Er and Tm from the regression coefficients. Using these γ's, we adjusted ΔG_1 and ΔG_2 for Gd, Tb, Dy and Er such that F^E_{gas}/F^{Sm}_{gas} calculated from ΔG_1, ΔG_2 and γ matched exactly the F^E_{gas}/F^{Sm}_{gas} value of B-32W. The ΔG_1 and ΔG_2 values for Tm were adjusted by the maximum amount allowed by the error bounds, but an exact match between observed and calculated Tm enrichments in B-32W could not be achieved. The adjustments to the free energies for this model are given in Table 2. A new set of F^E_{gas}/F^{Sm}_{gas} values as a function of temperature was calculated from γ^E, ΔG^E_1 and ΔG^E_2 using (11) and (12) for use in determining perovskite removal temperatures of other inclusions. Assuming that component 2 was uniformly enriched in all REE by a factor of 17.8, model enrichment factors and values for F_1, F_2, J_1 and M.D. were calculated in each group II inclusion in exactly the same way as in the two-component, ideal solution model. The predicted enrichment factors were almost exactly the same as those of the two-component, ideal solution model, the only differences being that slightly higher enrichments of Tm were predicted. The range of perovskite removal temperatures was wider and extended down to ~1600 K. The amount of component 2 in each inclusion was the same, so that the correlations between the Sm content calculated to be due to component 2 and Zr and Ir were the same. Two-component, non-ideal solution models in which different functional relationships between γ and ionic radius are used will also give almost exactly the same fits as the two-component, ideal solution model, as long as γ does not vary with temperature and ΔG's are adjusted within their error bounds to fit B-32W. Since the results of two-component, non-ideal solution models give only slightly better fits to Tm than those of the two-component, ideal solution model and the former models require larger adjustments to ΔG_1 and ΔG_2 than are required by the latter (Table 2), we continue to favor the two-component, ideal solution model.

Condensation of Eu and Yb

Both group II and group III inclusions contain large negative Eu and Yb anomalies relative to the light REE. In each inclusion, the magnitude of the Eu anomaly is similar to that of the Yb anomaly. In the few remaining inclusions whose heavy REE patterns resemble those of group II inclusions, referred to here as group IIA inclusions, Eu is enriched relative to the light REE by about the same amount as Yb. The correlation between Eu and Yb anomalies can be seen in Fig. 12, where Cl chondrite-normalized Eu/Sm and Yb/Sm ratios are plotted. Group II and group III inclusions probably had similar condensation histories, with the major difference

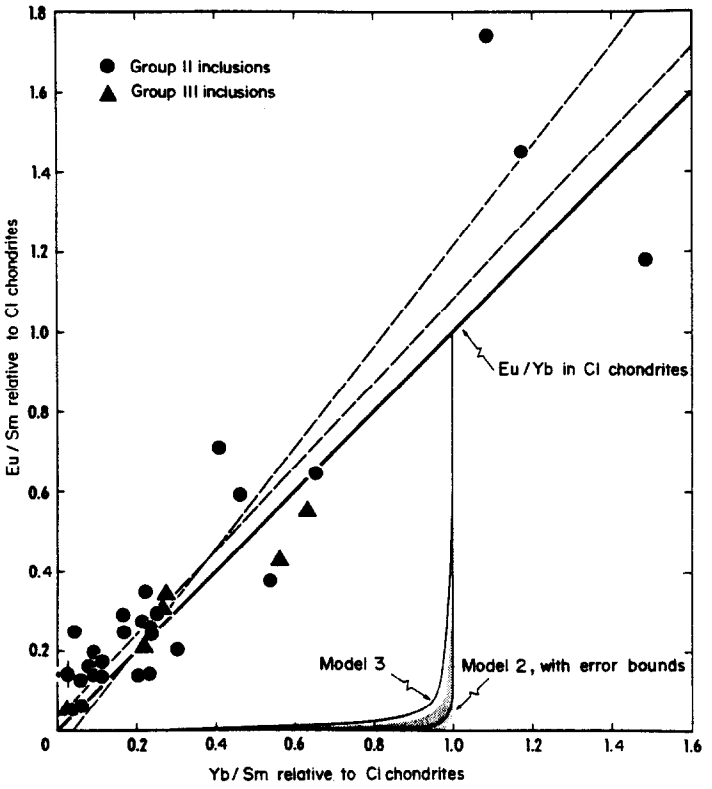

Fig. 12. Group II and III inclusions do not fall along the condensation trajectories for models 2 and 3 in a gas of solar composition.

being that the gas from which the group III inclusions formed did not experience removal of early condensates including perovskite and trace elements more refractory than perovskite. Eu and Yb are more volatile than the other REE and probably did not condense completely when group II and III inclusions condensed.

An excellent correlation between Eu/Sm and Yb/Sm ratios can be seen in Fig. 12. For the 34 inclusions that can be recognized as being members of group II, IIA or III, the correlation coefficient is +0.913 which is significant at greater than the 99.9% level. The slope of the correlation is nearly the same as the Eu/Yb ratio of Cl chondrites, with Eu/Sm and Yb/Sm ratios ranging from near zero to greater than those of Cl chondrites. Also plotted in Fig. 12 are condensate composition trajectories calculated for ideal solid solution of REE in perovskite, model 2, and for a non-ideal solid solution model, model 3, in which the perovskite activity coefficients are those used in the two-component, non-ideal solution model described in detail, above. Data for the inclusions do not lie along either condensation trajectory.

The behavior of Yb cannot be explained if the inclusions condensed from a gas of solar composition with the REE in either ideal or moderately non-ideal solid solution. The inclusions have J^{Yb}/J^{Sm} ratios as low as 0.026, while the J^{Yb}/J^{Sm} ratio of condensates in which REE have dissolved in ideal solid solution is greater than 0.064 at all temperatures. If the activity coefficients of model 3 are used, lower J^{Yb}/J^{Sm} ratios will result, but J^{Yb}/J^{Sm} ratios of less than 0.026 will be obtained only when F^{Sm}_{cond} is less than 0.67. Since the large amounts of spinel and volatile lithophile elements in fine-grained inclusions indicate near total condensation of Sm, moderately non-ideal solid solution condensation calculations will not explain the data either. Low J^{Yb}/J^{Sm} ratios in the condensate with near total condensation of Sm can be obtained if γ_{Lu}/γ_{Sm} ratios of greater than 100 are used, but we have shown that such large relative activity coefficients are unreasonable.

A more reasonable explanation is that the inclusions formed in a gas of somewhat more reducing composition than that of the standard solar gas. There are conditions under which the oxygen partial pressure is considerably lower, yet the major condensate phases are still oxides and silicates: C/O ~0.9 rather than C/O = 0.55 (solar composition). The dominant condensation reaction for Yb is

$$2\,Yb_{(g)} + 3\,O_{(g)} \rightleftarrows Yb_2O_{3(s)} \qquad \text{(R-6)}$$

while that for all other REE except Tm is

$$2\,LnO_{(g)} + O_{(g)} \rightleftarrows Ln_2O_{3(s)}. \qquad \text{(R-7)}$$

Thus, if the gas composition becomes more reducing, (R-6) will be driven more strongly to the left than (R-7) will be and Yb will become more volatile rela-

tive to Sm. Under these compositional conditions, low J^{Yb}/J^{Sm} ratios with high degrees of condensation of Sm will be permitted for a condensate in which REE dissolve in ideal solid solution. As discussed later in the paper, condensation from a reducing gas also provides much better agreement between calculated and observed Tm abundances, without affecting the degree of fit to the other REE.

Using this idea, there are two possible explanations for the correlation seen in Fig. 12. The first is that virtually no Eu and Yb condensed with the rest of the REE in component 1 and that both elements condensed totally in a volatile-rich component which brought in Eu and Yb later. The second is that the condensation temperatures of the inclusions are so low that the data plot near the condensation trajectory for component 1. If the C/O ratio were just right, the condensation trajectory could be coincident with the Cl chondrite Eu/Yb ratio reference line on Fig. 12. A wider range of C/O ratios would be permitted if Eu and Yb entered the inclusions in a separate volatile-rich component. We will model REE condensation from reducing gases in detail in a future paper.

CONCLUSIONS

Comparison of REE condensation models

Now that we know the properties of the one-component, non-ideal solution (model 1), two-component, ideal solution (model 2) and two-component, non-ideal solution (model 3) models, we will summarize their advantages and disadvantages.

Thermodynamic quantities. Model 1 requires activity coefficient ratios for solid solution of heavy REE in perovskite or any other host phase to change rapidly and irregularly with temperature. γ_{Lu}/γ_{Sm} for perovskite must increase by a factor of 400 over a 20° temperature range and must differ by as much as a factor of 20 to match different inclusions with virtually identical perovskite removal temperatures. Furthermore, perovskite-liquid partition coefficient experiments do not support γ_{Lu}/γ_{Sm} values substantially greater than 20, while some inclusions require γ_{Lu}/γ_{Sm} values well over 100 to be fit by model 1. Models 2 and 3 make no such excessive demands on the laws of thermodynamics, since they use a single, consistent set of free energies and activity coefficients to model all group II inclusions. The adjustments to free energies required to fit one inclusion, B-32W, are smaller in model 2 than in model 3.

Accuracy of fit to Gd, Tb, Dy, Ho, Er and Lu. Models 2 and 3 have virtually identical values of mean deviation (18) for every group II inclusion modelled. The mean deviations for models 1 and 2 are compared in Table 4. The mean deviations, averaged over 17 inclusions, are $11.4 \pm 1.6\%$ and $8.0 \pm 1.0\%$ for models 1 and 2, respectively. Examination of Table 4 shows that the larger average M.D. for model 1 is not caused by a single inclusion with a large M.D., but rather because model 2 very commonly provides better fits than model 1. Thus, models 2 and 3 are generally superior to model 1 in their ability to accurately predict enrichment factors for Gd, Tb, Dy, Ho, Er and Lu when large numbers of inclusions are modelled.

Other refractory elements. Both models 2 and 3 predict that there will be a correlation between the concentrations of elements more refractory than perovskite and the amount of Sm due to component 2. Furthermore, these models predict that the ratios of these refractory elements to the amount of Sm due to component 2 should be similar to the abundance ratios of these elements to Sm in Cl chondrites. Model 1 predicts that elements more refractory than perovskite will not be present in group II inclusions. The fact that these refractory elements are present in group II inclusions in the amounts predicted by models 2 and 3 argues strongly in favor of the latter models.

Tm anomalies. All three REE condensation models under consideration consistently underestimate the enrichment factor for Tm (Table 4). Model 1 predicts higher Tm enrichment factors than do models 2 and 3 and would predict still higher Tm enrichment factors if γ_{Sm} values greater than unity were used. Although correct Tm enrichment factors are calculated for some inclusions when γ_{Sm} values greater than unity are used in model 1, incorrect values would be calculated for the remaining inclusions. Models 2 and 3 predict that Tm has a volatility slightly less than and slightly greater than that of Gd, respectively, while group II inclusions behave as if Tm was considerably more volatile than Gd. Thus model 3 is slightly better than model 2 in its ability to model Tm, but neither is satisfactory.

We have considered three alternative explanations for the Tm anomalies. (1) Some nuclear process could have produced excesses compared to Cl chondrites in monoisotopic Tm relative to other REE isotopes in the region where the group II inclusions formed. This explanation is extremely unlikely, because nuclear effects of the magnitude necessary to produce the Tm anomaly would produce substantial isotopic anomalies in polyisotopic REE. REE isotopic anomalies have been found in two Allende inclusions, but the anomalous isotope ratios deviate from normal abundances by less than 1% (MCCULLOCH and WASSERBURG, 1978a,b; LUGMAIR *et al.*, 1978). Furthermore, nuclear production of excess Tm would not be expected to produce the consistently chondritic Tm/Sm ratio in group II inclusions. (2) There is a large error in the thermodynamic data for Tm. There is no support for this hypothesis other than the inability of three REE condensation models to correctly predict Tm concentrations in group II inclusions. (3) The group II inclusions did not form in a gas of solar composition. A preliminary investigation has shown that under reducing conditions, Tm becomes more volatile relative to the other heavy REE for the same reason that Yb becomes more volatile, i.e. Tm con-

denses predominantly according to a reaction of the same form as (R-6). This appears to be the most likely explanation for the Tm anomaly, especially since such gases also allow explanation for the behavior of Yb. REE condensation from non-solar gases will be investigated in detail in a separate paper.

Alternative models to explain REE patterns in group II inclusions. In this paper, we have examined in detail equilibrium condensation models to explain the REE patterns of group II inclusions and found that a minimum of two REE-bearing condensate components are required. One non-equilibrium condensation model, in which perovskite condensed extremely rapidly was investigated by BOYNTON (1975). In this model, only the outer surface of the perovskite is in equilibrium with the gas, so that the heavy REE patterns are more fractionated than those in a model in which the entire crystal is in equilibrium with the gas. Boynton found that in order to fit G_p with this non-equilibrium model, the relative activity coefficients would have to be twice as large as those for the equilibrium model. Since the problem in modelling group II inclusions is to explain why their heavy REE patterns are less fractionated than is indicated by equilibrium condensation with ideal solution, non-equilibrium models of this sort are not likely to lead to a solution of the problem. Other models can be envisioned in which the REE patterns of these inclusions are controlled by other non-equilibrium effects, such as variable diffusion rates of REE in condensate minerals, or by different thermodynamic properties of trace elements condensed on the surfaces of grains, but we have not investigated such models in detail.

Implications of the two-component model. By applying a thermodynamically reasonable model to the group II inclusions, we have found that removal of perovskite took place over a surprisingly narrow temperature range, that the gas-solid fractionations that affected the REE patterns of these inclusions probably took place in a gas of reducing composition and that at least two REE-bearing components are present in these inclusions. GROSSMAN *et al.* (1979) found that a component uniformly enriched in all refractory elements was necessary to explain the abundances of these elements in amoeboid olivine aggregates and supported the suggestion of GROSSMAN and STEELE (1976) that small fragments of coarse-grained inclusion material were present. We have now found that a similar refractory element-rich component is necessary to explain the REE patterns of group II inclusions. Thus, there seems to be a component, which may consist of fragments of coarse-grained inclusions, that contaminates lower temperature assemblages in Allende. We are searching for petrographic evidence for this component in fine-grained inclusions.

GROSSMAN *et al.* (1979) pointed out how the presence of both coarse- and fine-grained inclusions in Allende meant that the parent body of this meteorite sampled materials that condensed from separate nebular reservoirs. This was based on the fact that REE patterns of coarse-grained inclusions require total condensation of REE without fractionation while those of fine-grained inclusions require condensation after prior removal of the most refractory REE. The two-component model discussed in the present paper implies that at least some of this mixing occurred during formation of individual inclusions, prior to assembly of the Allende parent body. In fact, we now suspect that even the fine-grained inclusions themselves contain the two REE-bearing components which GROSSMAN *et al.* (1979) thought dominated the bulk Allende REE pattern. We cannot rule out the possibility that the two components present in the group II inclusions condensed from gases of different composition. The presence of rims on coarse-grained inclusions (WARK and LOVERING, 1977) also seems to imply inclusion formation by mixing of components which condensed from different reservoirs. Here again, gases of different composition may have been involved.

Acknowledgements—We are indebted to W. V. BOYNTON for motivating us to pursue this exhaustive investigation of REE condensation models. We are grateful to T. TANAKA, R. N. CLAYTON, R. C. NEWTON and D. WHITE for helpful discussions. We thank H. PALME and J. M. LATTIMER for permission to use unpublished data. The manuscript was typed by M. BOWIE. This work was supported by funds from the National Aeronautics and Space Administration through grant NGR 14-001-249 and from the Alfred P. Sloan Research Foundation.

REFERENCES

ACKERMANN R. J. and RAUH E. G. (1971) A high-temperature study of the stoichiometry, phase behavior, vaporization characteristics, and thermodynamic properties of the cerium + oxygen system. *J. Chem. Thermodynamics* **3**, 609–624.

ALLEN J. M., GROSSMAN L., DAVIS A. M. and HUTCHEON I. D. (1978) Mineralogy, textures and mode of formation of a hibonite-bearing Allende inclusion. *Proc. Ninth Lunar Planet. Sci. Conf.*, 1209–1233.

AMES L. L., WALSH P. N. and WHITE D. (1967) Rare Earths. IV. Dissociation energies of the gaseous monoxides of the rare earths. *J. Phys. Chem.* **71**, 2707–2718.

BORODIN L. S. and BARINSKII R. L. (1960) Rare earths in perovskites (knopites) from massifs of ultrabasic alkalic rocks. *Geochemistry* **4**, 343–351.

BOYNTON W. V. (1975) Fractionation in the solar nebula: condensation of yttrium and the rare earth elements. *Geochim. Cosmochim. Acta* **39**, 569–584.

BOYNTON W. V. (1978) Fractionation in the solar nubula, II. Condensation of Th, U, Pu and Cm. *Earth Planet. Sci. Lett.* **40**, 63–70.

CONARD R. (1976) A study of the chemical composition of Ca-Al-rich inclusions from the Allende meteorite. M.S. Thesis, Oregon State University.

CONARD R. L., SCHMITT R. A. and BOYNTON W. V. (1975) Rare-earth and other elemental abundances in Allende inclusions. Abstract. *Meteoritics* **10**, 384–387.

DAVIES O. L. and GOLDSMITH P. L. (1972) (eds) *Statistical Methods in Research and Production*, 4th edn. 478 p. Longman.

DAVIS A. M., ALLEN J. M. and GROSSMAN L. (1978a) Major and trace element characteristics of coarse-grained inclusions in Allende. Abstract. *EOS (Trans. Am. Geophys. Union)* **59**, 314.

DAVIS A. M., GROSSMAN L. and ALLEN J. M. (1978b) Major and trace element chemistry of separated fragments from a hibonite-bearing Allende inclusion. *Proc. Ninth Lunar Planet. Sci. Conf.*, 1235–1247.

DESOETE D., GIJBELS R. and HOSTE J. (1972) *Neutron Activation Analysis.* 836 p. Wiley-Interscience.

EVENSEN N. M., HAMILTON P. J. and O'NIONS R. K. (1978) Rare-earth abundances in chondritic meteorites. *Geochim. Cosmochim. Acta* **42**, 1199–1212.

GANAPATHY R., PAPIA G. M. and GROSSMAN L. (1976) The abundances of zirconium and hafnium in the solar system. *Earth Planet. Sci. Lett.* **29**, 302–308.

GOLDSTEIN H. W., WALSH P. N. and WHITE D. (1961) Rare earths. I. Vaporization of La_2O_3 and Nd_2O_3: dissociation energies of gaseous LaO and NdO. *J. Phys. Chem.* **65**, 1400–1404.

GOODENOUGH J. B. and LONGO J. M. (1970) Crystallographic and magnetic properties of perovskite and perovskite-related compounds. In *Landolt-Börnstein Numerical Data and Functional Relationships in Science and Technology* (eds K.-H. Hellwege and A. M. Hellwege), Group III, Vol. 4, Part a, pp. 126–314. Springer-Verlag.

GROSSMAN L. (1972) Condensation in the primitive solar nebula. *Geochim. Cosmochim. Acta* **36**, 597–619.

GROSSMAN L. (1975) Petrography and mineral chemistry of Ca-rich inclusions in the Allende meteorite. *Geochim. Cosmochim. Acta* **39**, 439–454.

GROSSMAN L. and GANAPATHY R. (1976a) Trace elements in the Allende meteorite—I. Coarse-grained, Ca-rich inclusions. *Geochim. Cosmochim. Acta* **40**, 331–344.

GROSSMAN L. and GANAPATHY R. (1976b) Trace elements in the Allende meteorite—II. Fine-grained, Ca-rich inclusions. *Geochim. Cosmochim. Acta* **40**, 967–977.

GROSSMAN L. and STEELE I. M. (1976) Amoeboid olivine aggregates in the Allende meteorite. *Geochim. Cosmochim. Acta* **40**, 149–155.

GROSSMAN L., GANAPATHY R. and DAVIS A. M. (1977) Trace elements in the Allende meteorite—III. Coarse-grained inclusions revisited. *Geochim. Cosmochim. Acta* **41**, 1647–1664.

GROSSMAN L., GANAPATHY R., METHOT R. L. and DAVIS A. M. (1979) Trace elements in the Allende meteorite —IV. Amoeboid olivine aggregates. *Geochim. Cosmochim. Acta* **43**, 817–829.

GSCHNEIDNER K. A. JR, KIPPENHAN N. and MCMASTERS O. D. (1973) Thermochemistry of the rare earths. Part I. Rare earth oxides. Report IS-RIC-6, Rare-Earth Information Center, Ames, Iowa.

HASKIN L. A., FREY F. A., SCHMITT R. A. and SMITH R. A. (1966) Meteoritic, solar and terrestrial rare-earth distributions. In *Physics and Chemistry of the Earth* (eds L. H. Ahrens, F. Press, S. K. Runcorn and H. C. Urey). Vol. 7, pp. 167–321. Pergamon Press.

HULTGREN R., ORR R. L. and KELLY K. K. (1964 and later) Selected values of thermodynamic properties of metals and alloys. Supplements. University of California, Berkeley, California.

JANAF Thermochemical Tables (1977) Supplement No. 47. Compiled by the Thermal Research Laboratory, Dow Chemical Company, Midland, Michigan.

KRÄHENBÜHL U., MORGAN J. W., GANAPATHY R. and ANDERS E. (1973) Abundance of 17 trace elements in carbonaceous chondrites. *Geochim. Cosmochim. Acta* **35**, 337–363.

LATTIMER J. M., SCHRAMM D. N. and GROSSMAN L. (1978) Condensation in supernova ejecta and isotopic anomalies in meteorites. *Astrophys. J.* **219**, 230–249.

LUGMAIR G. W., MARTI K. and SCHEININ N. B. (1978) Incomplete mixing of products from r-, p- and s-process nucleosynthesis: Sm-Nd systematics in Allende inclusion Ek 1-04-1. In *Lunar and Planetary Science* IX, pp. 672–674.

MARTIN P. M. and MASON B. (1974) Major and trace elements in the Allende meteorite. *Nature* **249**, 333–334.

MASON B. and MARTIN P. M. (1977) Geochemical differences among components of the Allende meteorite. *Smithson. Contrib. Earth Sci.* No. 19, pp. 84–95.

MCCULLOCH M. T. and WASSERBURG G. J. (1978a) Barium and neodymium isotopic anomalies in the Allende meteorite. *Astrophys. J. Lett.* **220**, L15–L19.

MCCULLOCH M. T. and WASSERBURG G. J. (1978b) More anomalies from the Allende meteorite: samarium. *Geophys. Res. Lett.* **5**, 599–602.

NAGASAWA H., BLANCHARD D. P., JACOBS J. W., BRANNON J. C., PHILPOTTS J. A. and ONUMA N. (1977) Trace element distribution in mineral separates of the Allende inclusions and their genetic implications. *Geochim. Cosmochim. Acta* **41**, 1587–1600.

NAGASAWA H., SCHREIBER H. D. and BLANCHARD D. P. (1976) Partition coefficients of REE and Sc in perovskite, melilite, and spinel and their implication for Allende inclusions. In *Lunar Science* VII, pp. 587–589.

NAKAMURA N. (1974) Determination of REE, Ba, Fe, Mg, Na and K in carbonaceous and ordinary chondrites. *Geochim. Cosmochim. Acta* **38**, 757–775.

RINGWOOD A. E. (1975) Some aspects of the minor element chemistry of lunar mare basalts. *Moon* **12**, 127–157.

SHANNON R. D. (1976) Revised effective ionic radii and systematic studies of interatomic distances in halides and chalcogenides. *Acta Cryst.* **A32**, 751–767.

TANAKA T. and MASUDA A. (1973) Rare-earth elements in matrix, inclusions, and chondrules of the Allende meteorite. *Icarus* **19**, 523–530.

WARK D. A. and LOVERING J. F. (1977) Marker events in the early evolution of the solar system: evidence from rims on Ca-Al-rich inclusions in carbonaceous chondrites. *Proc. Eighth Lunar Sci. Conf.*, 95–112.